www.bre.co.uk

Solid wall heat losses and the potential for energy saving

In situ U-value measurement method review

Prepared for: Dr Elizabeth Milsom

Date: 06 July 2016

BRE
Watford, Herts
WD25 9XX

Customer Services 0333 321 8811

From outside the UK:
T + 44 (0) 1923 664000
F + 44 (0) 1923 664010
E enquiries@bre.co.uk
www.bre.co.uk

bre

Notes

This report is part of a collection of outputs from the DECC research project investigating the savings achieved with the installation of solid wall insulation. These will be made available on the project web site where a summary of the project can also be found (see http://www.bre.co.uk/swi).

The lead authors for this report were Tim Ward and Sean Doran of BRE.

bre

Executive Summary

Field trials have produced results which suggest that U-values of solid walls are lower than currently assumed. The standard methodology for in situ U-value measurement is described in ISO 9869: 1994 "*Thermal insulation – In situ measurements of thermal resistance and thermal transmittance".* This report considers whether the method used for measuring U-values in situ produces sufficiently accurate results.

The methodology for assessing in situ U-value measurements consisted of seven tests in both laboratory and field settings. These are:

1. The comparison of the in situ method with hot-box measurements
2. The impact of surface roughness on accuracy
3. Reproducibility of the substrate to the heat flow sensor
4. The method of affixing the sensor to a wall
5. The impact of direct sunlight on a measured U-value
6. Stratification of indoor temperature with respect to height
7. Stratification of indoor temperature with respect to distance from wall

Tests 1 and 2 showed that the U-values obtained using the in situ HFP methodology compared well with those obtained using the hot-box methodology but that a small systematic error exists in the measured heat flows. It is therefore reasonable to make a correction to the heat flows (and hence determined U-values) measured.

Tests 3 to 7 looked at the practical aspects of the methodology. They sought to understand more about the validity of commonly used techniques and their constraints.

Taken together, these tests can be considered to have validated the technology used to measure in situ U-values; namely the HFP01 heat flux plates and associated equipment, as well as the methodology used to undertake measurements. More is now known about the constraints of the method; such as its use in summer months, and of its components; such as the positioning of temperature sensors.

bre

Table of Contents

bre

1 Introduction

Several field trials, including the 2011 field trial undertaken by BRE, have produced results which suggest that U-values of solid walls are lower than currently assumed. Similar techniques based around the same measurement methodology (ISO 9869: 1994 "*Thermal insulation – In situ measurements of thermal resistance and thermal transmittance*") were used for each of these trials and this methodology now requires validation in case of any systematic bias or other deficiency in the procedure. Two explanations exist for this apparent discrepancy between measured and calculated U-values for solid walls: Either the method and set-up of measuring U-values in situ is producing incorrect values, or the base assumptions underlying the calculation of the U-values are in some way incorrect (perhaps because of an unknown characteristic of the wall). This report considers the first of these; whether the method used for measuring U-values in situ produces sufficiently accurate results. A subsequent paper in this report series will consider the methodology and assumptions used to calculate U-values.

The methodology for assessing in situ U-value measurements consisted of seven tests in both laboratory and field settings. These are:

1. The comparison of the in situ method with hot-box measurements
2. The impact of surface roughness on accuracy
3. Reproducibility of the substrate to the heat flow sensor
4. The method of affixing the sensor to a wall
5. The impact of direct sunlight on a measured U-value
6. Vertical stratification of indoor temperature
7. Horizontal stratification of indoor temperature

Tests 1 & 2 were carried out in NPL's (National Physical Laboratory) rotatable hot-box, tests 3 to 7 were carried out in a vacant dwelling with a controlled indoor environment. These tests have been designed to interrogate all major aspects of the in situ measurement methodology and the aim is that the results presented here should indicate the degree of confidence that should be placed in measurements made using the method investigated.

Heat flux (W/m^2) is, under steady-state conditions, proportional to the difference in temperature between the inside and outside of a building element such as a wall or roof. The thermal performance of a building element (such as a wall, for example) is normally expressed as a U-value which under steady state conditions is the heat flux (W/m^2) divided by the temperature difference (K) between the internal and external environments.

In situ, the temperatures either side of the building element are not steady state and so the measured U-value is equal to the mean heat flux through the building element divided by the mean temperature difference across it, provided these mean values are evaluated over a sufficiently long period of time in order to deal with thermal storage effects where some of the heat is stored by or released from within the particular building element.

In situ heat flux through walls is monitored using heat flux plates (hereafter HFPs) and readings are typically recorded every 15 minutes using dataloggers. Temperatures are measured using thermistors and in most cases they are recorded using the same loggers. Where it is impossible to measure external temperatures using wired thermistors, small independent temperature loggers are used.

The data obtained from monitoring is used to derive measured U-values. The U-values are normally then interpreted, taking into account field observations and conventional methods of calculating U-values using British Standard BS EN ISO 6946.

The HFPs used for this work are the HFP01; manufactured by Hukseflux Thermal Sensors. The loggers used are Eltek Squirrel datalogggers. External temperature sensors (where used) are manufactured by Gemini Tinytag.

Since the field work involved occupied dwellings, the methodology was designed to measure U-values without damaging internal furnishings or endangering occupiers. HFPs were supported using an arrangement, developed for this purpose, involving adjustable poles and flexible clamps. A flexible substrate was applied to the HFPs to provide good thermal contact between the HFP and the internal surface of the wall.

bre

2 Tests 1 and 2 – The hot-box tests

This set of laboratory measurements was carried out in the rotatable hot-box rig at the National Physical Laboratory (NPL). The tests were designed to validate the use of the Hukseflux HFP01 heat flux plates (HFPs), which are commonly used for this kind of in situ measurement and which have been used in this project for measuring U-values of solid walls in situ and to determine the magnitude of any systematic error that might arise from their use. In order to achieve this the thermal performance of a test panel (under steady state conditions) was determined from the temperatures and heat flows obtained via the NPL hot-box method and this was compared to the thermal performance determined using the same hot-box temperatures, but using the heat flows as measured by five Hukseflux HFP01 HFPs, pressure-fixed to the hot-side surface of the test panel. This was repeated with embossed wallpaper applied to the hot side of the test panel to examine the effect that a rough surface has on the ability of the HFPs to measure heat flow.

Separately, the temperatures measured by thermistor temperature sensors (as used for the in situ field measurements) were recorded and compared to the air and radiant temperatures as measured by the NPL temperature sensors. This was to determine how close to air temperature these sensors measure.

In addition, thermal modelling of both the calibration set-up and the in situ set-up of the HFPs was carried out to investigate theoretically the behaviour of the Hukseflux HFP01 HFPs under these two different set-up conditions; and so determine separately the systematic error that is expected to be operating with the in situ measurement of heat flux (using HFP01 HFPs) and hence provide the magnitude and sign of the correction that should be applied to the heat flow measurements made in situ using HFP01 HFPs pressure-fixed to the inside surface of walls.

Finally, from other Hot-box tests (using another NPL Hot-box), runs on a particular built-wall (Wall 3) steady state and dynamic results were compared.

2.1 Design of the test panel

Figure 1 - 'Cold-side' of NPL hot-box test element showing the inserted test panel

The test panel, which measured 1.48m high x 1.23m wide, was inserted into the test opening in the expanded polystyrene surround of the hot-box testing element. The cold-side of the hot-box test element is shown in Figure 1. The recess depth of the test panel on the hot-side is identical to that of the cold side. The test panel consists of a 13mm thick layer of high density expanded polystyrene with 12.5mm plasterboard bonded to each face using PVA wood glue and an array of nine 6mm diameter nylon bolts. The thermal resistance of the test panel, the detail of which is given in Appendix A, plus standard surface resistances, gives a calculated U-value of 1.41 W/m²K. Figure 2 shows the dimensions of the test panel and the locations of the constructional nylon bolts and the five heat flux plates. Figure 3 shows a cross section schematic of the test panel in the hot-box with the HFPs installed and held in place by means of the pressure fixing arrangement. The detail of the pressure fixing of the heat flux plates can be seen more clearly in the images in Figure 4.

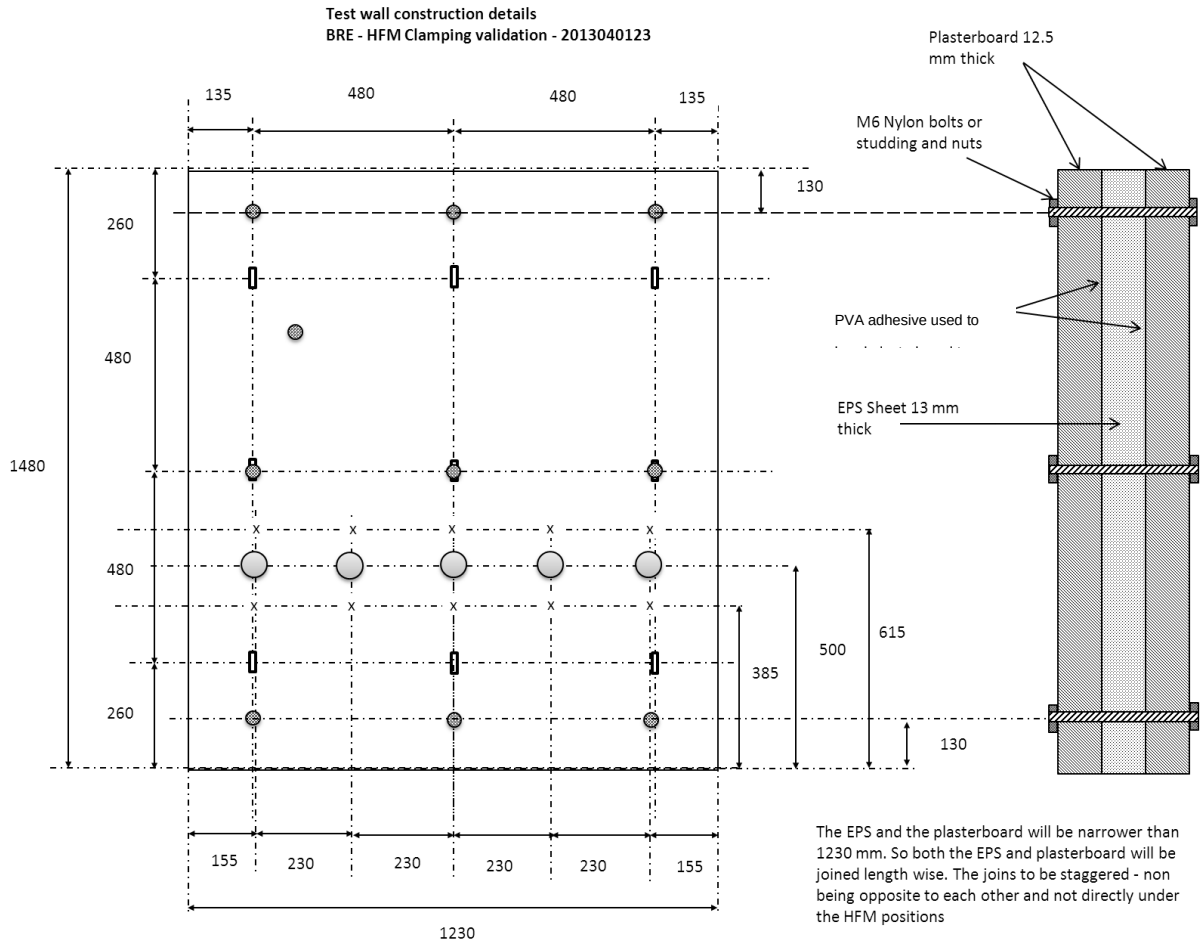

Figure 2 - Details of the construction of the test panel and the locations of the nylon bolts and the five heat flux sensors (row of larger circles)

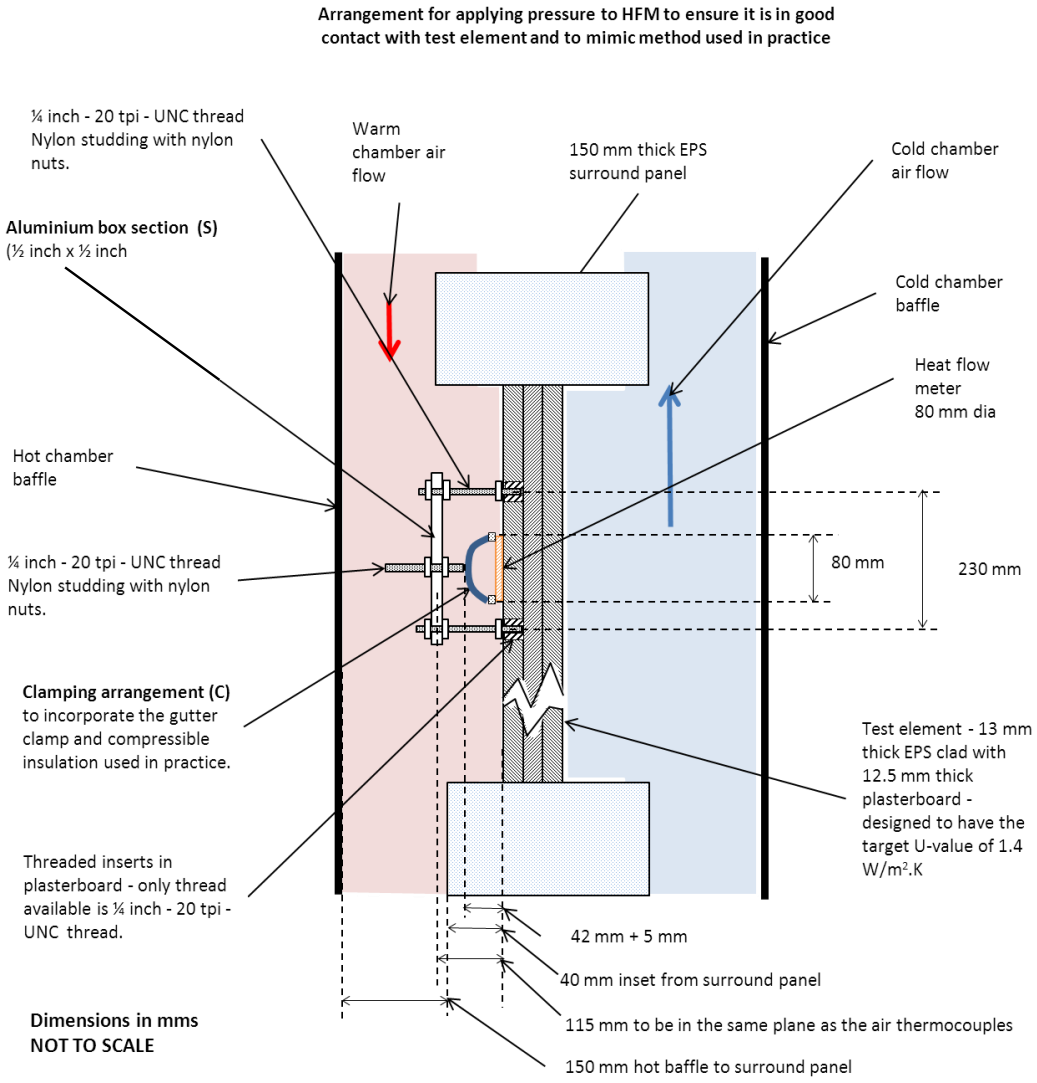

Figure 3 - Schematic cross-section through hot-box rig and test panel showing the pressure fixing system for the heat flux sensors

Figure 4 - Images of the heat flux sensors pressure fixed to the wall

2.2 Hot-box test runs

The description and objective for each of the five experimental runs on the test panel are given in Table 1 The NPL reference for each run is also given as an additional identifier. Run 2 included five thermistor temperature sensors (one for each heat flux plate position) where these were located close (approximately 20mm) to the HFP surface. They were positioned as they would be for in situ field measurements and were logged by the BRE logger used for in situ measurements. Run 3 had the same five thermistor temperature sensors, but moved away from the recessed test panel surface to be in the plane of the NPL air temperature measurements, i.e. in the undisturbed free flowing air across the surface of the hot-box test panel.

Table 1: Experimental runs on the test panel

Run Number (NPL Ref.)	Summary of test run and measurements made	Objective
Run 1 (R153A)	Measurement without heat flux plates in place. The test panel is constructed to represent a solid wall with known thermal resistance. It is designed to provide a U-value of approximately 1.4 W/m²K.	This test run is to determine the U-value of the test panel as measured by the hot box in the absence of the heat flux apparatus (in case this has a significant effect).
Run 2 (R153D)	Measurements with five heat flux plates placed in a line horizontally on the warm-side of the test panel	Compares the thermal performance measured by the in situ method with that determined from the hot box results
Run 3 (R153E)	As Run 2 but with four of the five heat flux plates rotated around the central heat flux plate	Examines whether the particular location of the heat flux plates has any effect on the results
Run 4 (R153F)	As Run 2 but with embossed wallpaper on ‘wall’ surface.	Examines the effect of a potentially poor thermal contact between ‘wall’ and heat flux plate
Run 5 (R153G)	As Run 3 but with embossed wallpaper on wall	As in Run 3.

The pressure-fixing system used with the HFP was developed for use in situ in occupied properties in order to avoid damaging the surface décor. It is essential with any fixing system to ensure a good thermal contact between the HFP and the surface of the plane element under test. This is achieved by having a thin layer of petroleum jelly on the underside of the HFP and a protective layer of polythene cling-film between this and the surface of the element under test. Figure 5 shows a close-up image of the HFP pressure-fixed to the test panel in Run 2 (where the surface finish is plasterboard) and an image of the underside of the HFP when it has been removed after completion of the test run.

The image of the underside of the HFP on removal from the plasterboard surface (right hand image of Figure 5), shows the relatively small indents in the plasterboard surface, indicating that there is complete thermal contact between the wall surface and the cling-film and hence the HFP.

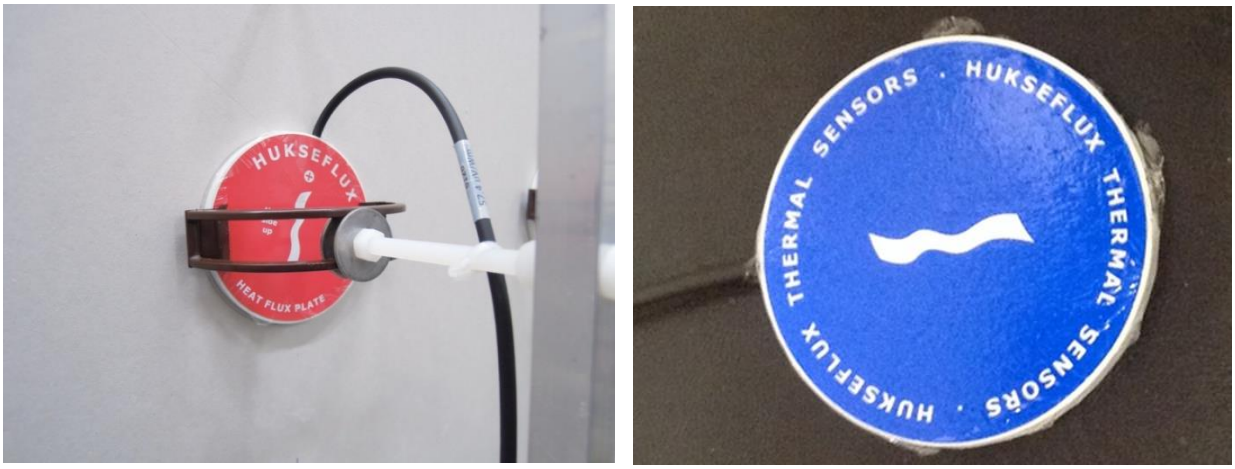

Figure 5 - Image of a HFP pressure-fixed to the plasterboard surface of the test panel and image of the underside of the sensor when removed

Figure 6 - Image of wallpapered surface and image of underside of HFP prior to install

Figure 6 shows an image of the test panel having been wallpapered on the hot-side and an image of the application of the petroleum gel prior to pressure fixing. The petroleum gel is a greater thickness initially, but under the pressure of the fixing system 'flows' to the edges of the HFP. Figure 7 shows a close-up image of the embossed wallpaper surface that applies to Runs 4 and 5, together with an image of the underside of a HFP on removal from the surface. It can be seen that the petroleum gel has indeed flowed to the edges of the HFP disc and importantly that both the small dimpled areas between leaves in the pattern and the very much larger and severe indents of the leaves themselves are clearly visible in the image, again indicating complete thermal contact of the cling-film and HFP, even in the case of a heavily embossed (or indented) surface.

Figure 7 - Image close-up of embossed wallpapered surface of the test panel for Runs 4 and 5 and an image of the underside of the HFP after removal

Thus, for the pressure-fix system used, there is good thermal contact between both smooth (plasterboard) and embossed (or indented) surfaces and the cling-film and HFP.

This gives confidence that in situ, there is likely to be good thermal contact between the surface and the HFP that is pressure-fixed in this way, regardless of that surface being smooth or embossed (or indented).

2.3 Results from the hot-box tests

2.3.1 Thermal performance of the test panel as measured by the NPL hot-box

The thermal performance of the test panel, as determined by the NPL hot-box method for each test run, is summarised in Table 2. These values are obtained from the average heat flows and average temperatures over a period of approximately 8 hours, when these heat flows and temperatures are close to steady state (see Figure 8 and Figure 9). The temperature sensors that relate to the test panel (both on the hot-side and cold-side) are equally spaced in three rows of three. For each of the nine locations the sensors measure air temperatures and radiant temperatures (i.e. baffle temperatures) opposite the test panel and surface temperatures of the test panel itself. Figure 10 shows a temperature map of these typical average temperatures for Run 2. In Figure 10 the location in each diagram of the numbered values (of air, radiant and surface temperatures) indicate the relative locations of the various sensors in the hot-box. The nine locations that are relevant to the test panel are inside the central rectangular 'box'. The values of R_{si} and R_{se} in Table 2 are determined from the average heat flow and the difference in temperature between the environmental temperature and the surface temperature. These various surface resistances are close to the standardised surface resistances of 0.13 and 0.04 m²K/W, respectively, for internal and external vertical surfaces (horizontal heat flow).

Run 1 is with no heat flux plates and no pressure fixing rigs. The base thermal performance of the test panel is determined from this run and the U-value is measured to be 1.41 W/m²K, which to three significant figures is the same as the calculated U-value (see Appendix A). Thus we have very good agreement between the U-value of the test panel measured by the hot-box apparatus and the calculated U-value.

Similarly, within the accuracy of the measured thermal conductance of the test panel of 1.852 W/m²K , this value is also in agreement with the calculated thermal conductance of 1.859 W/m²K of the test panel (see also Appendix A).

Table 2: Summary of measured thermal performance of the test panel

	Thermal values of the test panel based on averaged heat flow and averaged temperatures measured by the hot-box			
Run number	U-value (W/m²K)	Conductance (W/m²K)	R_{si} (m²K/W)	R_{se} (m²K/W)
1	1.41	1.852	0.124	0.045
2	1.41	1.856	0.123	0.045
3	1.42	1.863	0.122	0.044
4	1.40	1.835	0.123	0.045
5	1.41	1.840	0.122	0.044

Note: U-value includes R_{si} and R_{se}. Conductance excludes R_{si} and R_{se}

2.3.1.1 Influence of the heat flux plates on the total heat flow through the test panel

From thermal modelling of the HFP01 on the hot-side surface of the test panel (see 2.4.3 later), the presence of the HFP disturbs the heat flow through the test panel being measured. The net effect of this is in fact to add an additional heat flow of approximately 0.00029 W/K per HFP because of additional heat flow into the edges of the HFP. For the area of the test panel this increases the heat flow (through the test panel) by 0.01 % and hence the hot-box measured U-value of the test panel (with the five HFPs present) is also 0.01% higher than would have been the case with no HFPs present. However, this increase in measured U-value is well within the stated accuracy of ± 5.5% for the hot-box measurements. For example, for the hot-box measured U-values of around 1.41 W/m²K for the test-panel, this small increase in measured heat flow would result in no change in the second decimal and at most a change of

2 in the fourth decimal of the various measured U-values for the test-panel. Thus the effect of the presence of the five HFPs can readily be ignored and no correction need then be made to the various hot-box measured U-values.

2.3.1.2 Unadjusted comparison of heat flux measured by the HFP and hot-box

Although the presence of the HFPs adds to the heat flow through the test panel as just described in 2.3.1.1, the heat flux measured by the HFPs is in fact less than the undisturbed heat flux through the test panel. This is confirmed by thermal modelling (see 2.4.3 later) and is also demonstrated by comparing the hot-box measured heat flow to the unadjusted or 'raw' heat flows measured by the HFPs. Figure 8 and Figure 9 are, respectively, for Run 2 (plasterboard surface) and Run 4 (wallpaper surface). They are plots (over 8 hours of steady-state data at the end of each run) of the heat flux through the entire test panel (determined by the hot-box measurement) and the unadjusted heat flux through the test panel as measured directly by the five heat flux plates. This 'raw' HFP data gives both the variation in heat flux between the five heat flux plates and the proximity (or otherwise) to the average heat flux determined from the hot-box measurement. Using this raw measured heat flux, i.e. without any adjustment of the heat flux, what is noticeable in both graphs is that the heat flux measured by the HFP is generally less than the heat flux measured by the hot-box. In the case of the plasterboard surface (Figure 8) the mean of the HFP fluxes is about 6% less than that of the hot-box flux and in the case of the wallpaper surface (Figure 9) the mean is about 8% less than that of the hot-box heat flux. The variation in measured heat flux (between the different heat flux plates) is about ±5% in the case of the plasterboard surface and about ±8% in the case of the wallpaper surface. Some of this reduced heat flux measured by the HFP is due to the disturbance of the heat flux by the presence of the HFP itself. However, the behaviour of the HFP in measuring the heat flux requires some further refinement in order to take into account any local variations in temperature at the HFP locations on the hot-side surface of the test-panel in the hot-box and also any further systematic error that might arise from any differences in heat flux through the HFP under the different set-ups of calibration and in situ *use* (see 2.4.4 later).

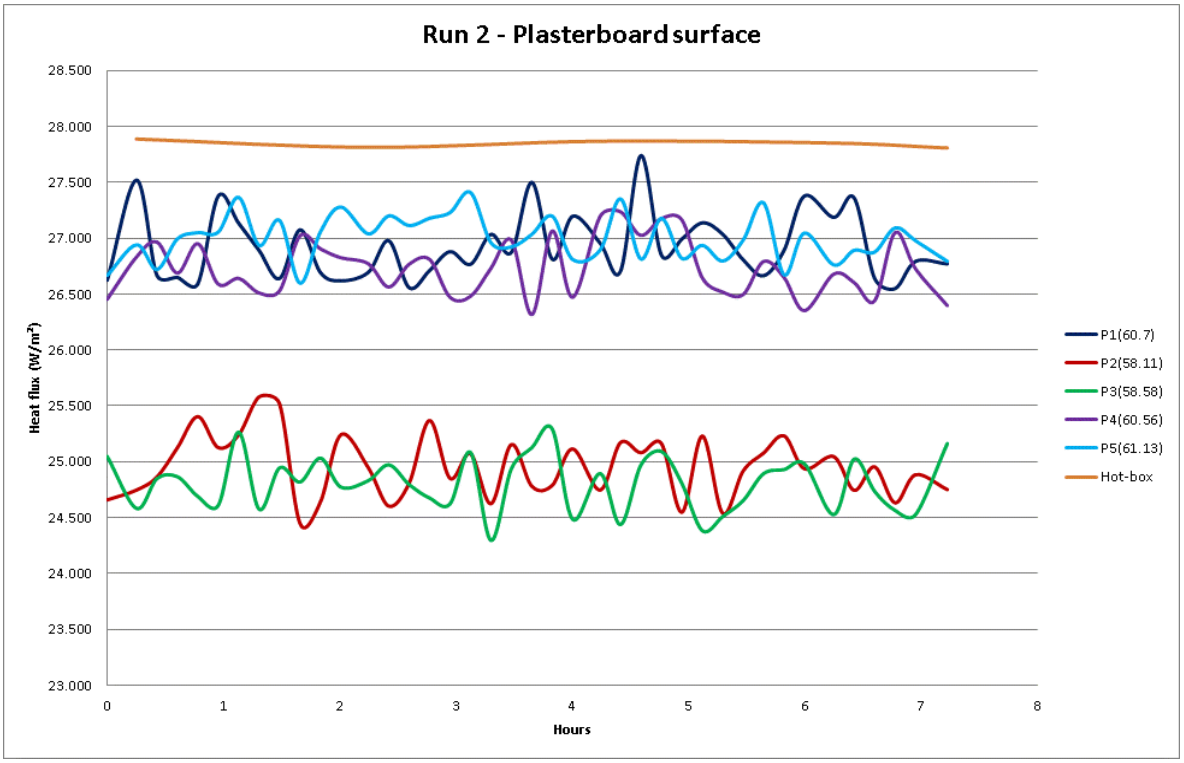

Figure 8 - 'Raw' heat fluxes (through test panel) for Run 2 (Plasterboard surface)

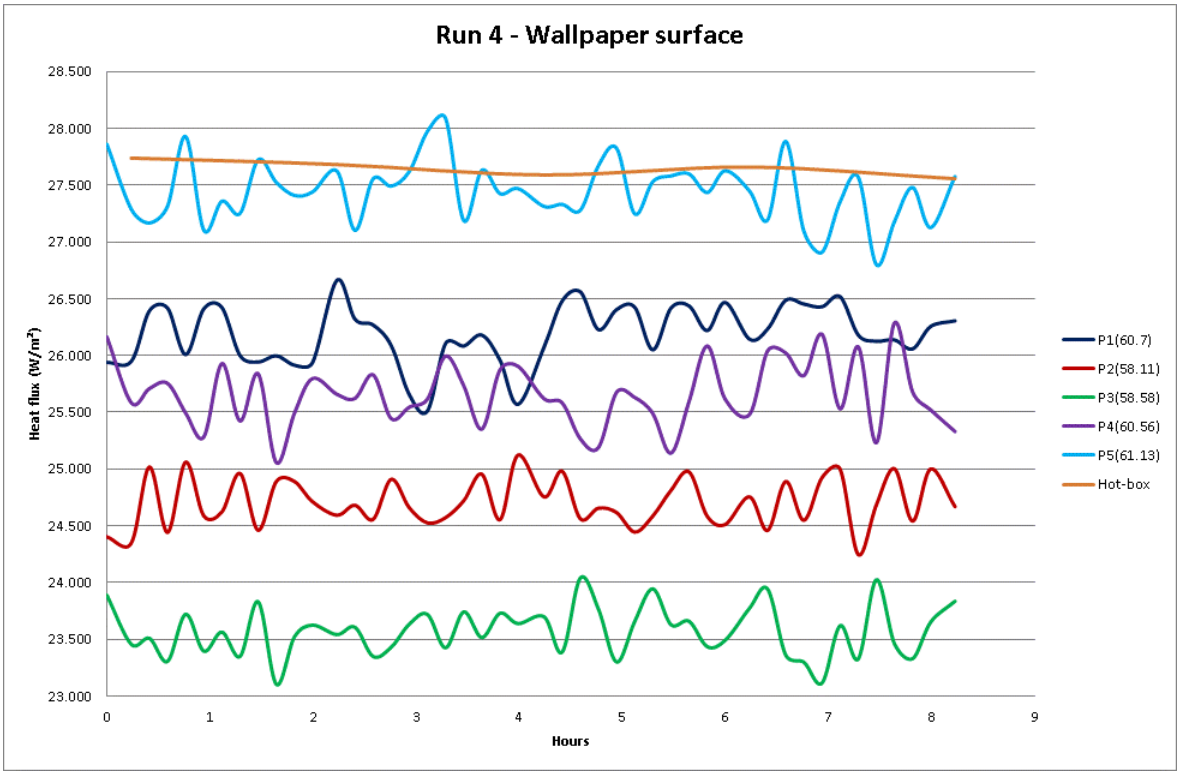

Figure 9 - 'Raw' heat fluxes (through test panel) for Run 4 (Wallpaper surface)

2.3.2 Validation of the thermal performance of the test panel measured by the heat flux plates

In order to validate the thermal performance of the test panel measured by the heat flux plates, the measured heat flux through the heat flux plates needs to be thoroughly understood. This section gives the detailed understanding of the behaviour of these heat flux plates in measuring heat flux.

2.3.2.1 Calibration uncertainty of the heat flux plates

The first important aspect of the HFPs to consider is the uncertainty in the calibration constant of the heat flux plates themselves. The heat flux plates used are made by Hukseflux, in the Netherlands. Each HFP manufactured is individually calibrated using a method developed by Hukseflux, where results from their calibration method (referred to as Hukseflux HFPC) have been checked against the results from a guarded hot-plate (Taurus TPL 300 DT) calibration system, carried out in accordance with the ASTM C1130 standard. The uncertainty in the calibration factor obtained from the Hukseflux HFPC calibration system is estimated (by Hukseflux) to be ±3% and the comparison between the Hukseflux HFPC and Taurus TPL 300 DT calibrations is within ±1%. Hukseflux estimate the total uncertainty of their calibration to be within ±5%, based on the standard uncertainty multiplied by a coverage factor of k=2, providing a level of confidence of 95%.

There is some dependence of the calibration factor on the mean temperature of the HFP, but this is small and amounts to only ±0.05% per ºK temperature difference between the calibration temperature of 21ºC and the in use mean temperature of the HFP. In comparing the HFP under calibration and in use in the hot-box, the mean temperature of the HFP is within one or two degrees kelvin and in this case the temperature correction is no more than 0.1% and so need not be applied. A realistic temperature range for the mean temperature of the HFP01 in situ is between 15ºC and 25ºC, corresponding to a temperature correction of approximately ±0.25%. This is small in the context of the overall accuracy of

around ±15% for in situ U-value measurement, so a correction for temperature would not normally be applied[1].

2.3.2.2 Variation of temperatures across the test panel

The array of temperatures used to determine the thermal values given in Table 2 are from specific points on the hot and cold sides of the test panel. There are nine locations in all and these are positioned in a regular grid (three by three), where each grid location represent equal areas of the test panel surface. This is precisely what is wanted for determining the thermal parameters of the test panel as a whole, however, there is in fact some variation in temperature across the face of the test panel and Figure 10 shows typical schematic temperature 'maps' (across the hot and cold sides of the hot-box) of air, radiant (baffle) and surface temperatures.

[1] In situ measurements are not normally steady state and indeed the internal temperature and hence the mean temperature of the HFP will vary. It can be argued that, strictly, the heat flux measured by the HFP should be adjusted. However, the correction that could be made will also be small at approximately ±0.25% for a variation in mean temperature of ±5ºK.

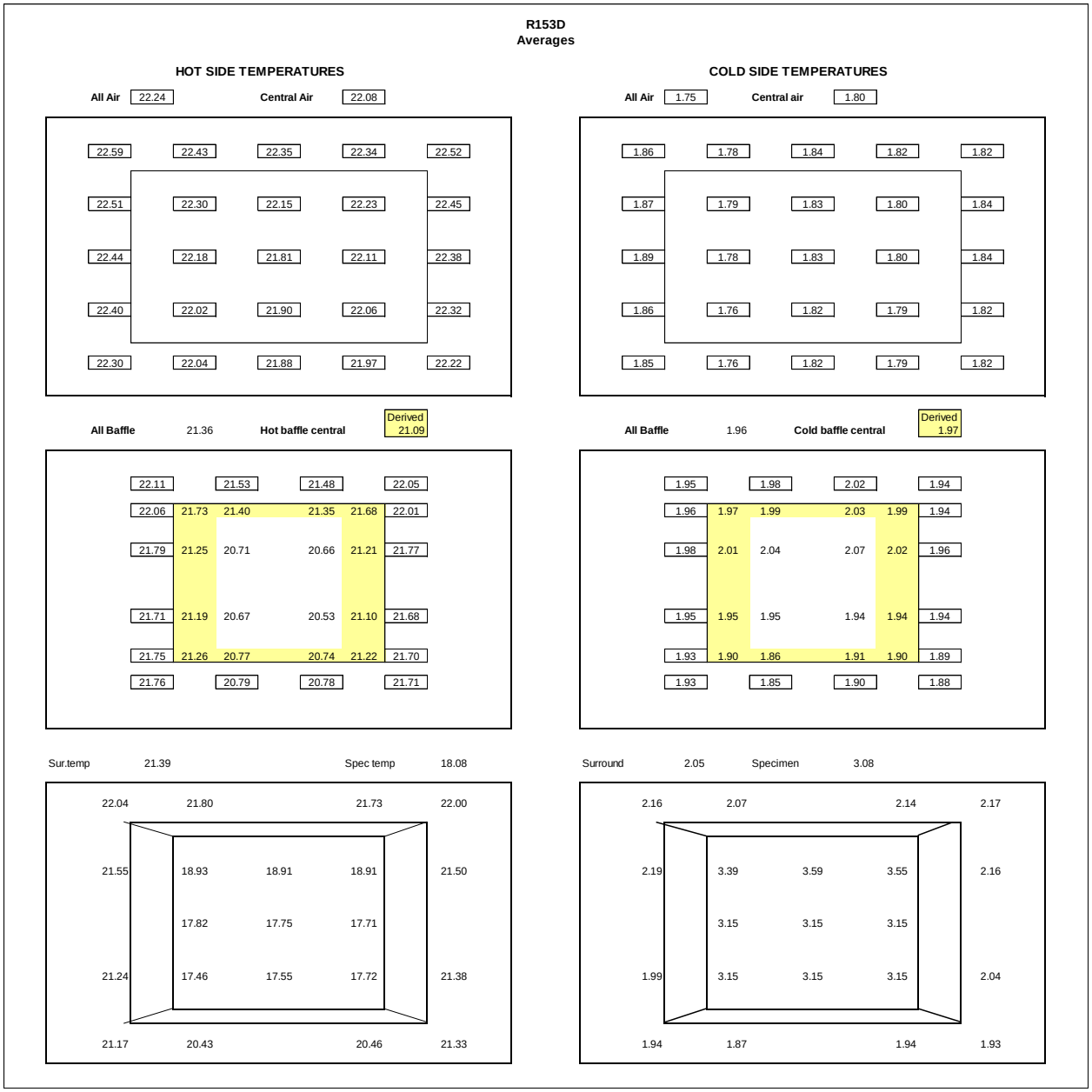

Figure 10 - Schematic 'maps' of typical average temperatures on either side of the hotbox. The outer 'box' represents the NPL hot-box testing element and the central box represents the test panel in the aperture of the testing element

2.3.2.3 Variation in air temperature close to the test-panel surface as measured by the thermistor sensors

Thermistor air temperature sensors (as used for in situ measurements) were also installed close (~20 mm) to the surface at each of the five heat flux plates in Runs 2 and 5. The thermistor sensors are encased in a polished metal tube. A close-up of the sensor (as mounted for Run 2) is shown in Figure 11. This thermistor sensor will normally respond to a particular mixture of the air temperature and the mean radiant temperature of the surrounding surfaces. The low emissivity of the polished metal tube of the sensor will significantly reduce the effect of any radiant temperatures, such that the temperature sensed by the thermistor should be close to the actual air temperature.

Figure 11: Thermistor sensor (metal-tube) mounted close to the HFP surface

From these, it was discovered that the air temperature in the recess of the test-panel was less than that in the free flowing air stream (115 mm from the surface). This is over and above the variation in the air temperature across the hot-side of the test panel shown in Figure 10. These air temperatures are plotted in Figure 12, together with the air and radiant temperature (seen by the hot-side surface of the test panel).

In Figure 12, comparing the five thermistor 'air' temperatures to (a) the air temperature and (b) the radiant temperature measured by the hot-box in Run 2, it can be seen that the measured 'air' temperatures are all lower than the hot-box air temperature, but also that the 'air' temperatures measured by the different HFPs also vary somewhat from location to location. For Run 3 however, the thermistor 'air' temperature sensors were positioned in the undisturbed air stream, and it can be seen that all the 'air' temperatures measured by the thermistor sensors hardly vary at all and that the mean of the five thermistor temperatures also now agrees with the hot-box air temperature. The important conclusion from this test is that the thermistor temperature sensor with its polished metal tube measures very close to air temperature.

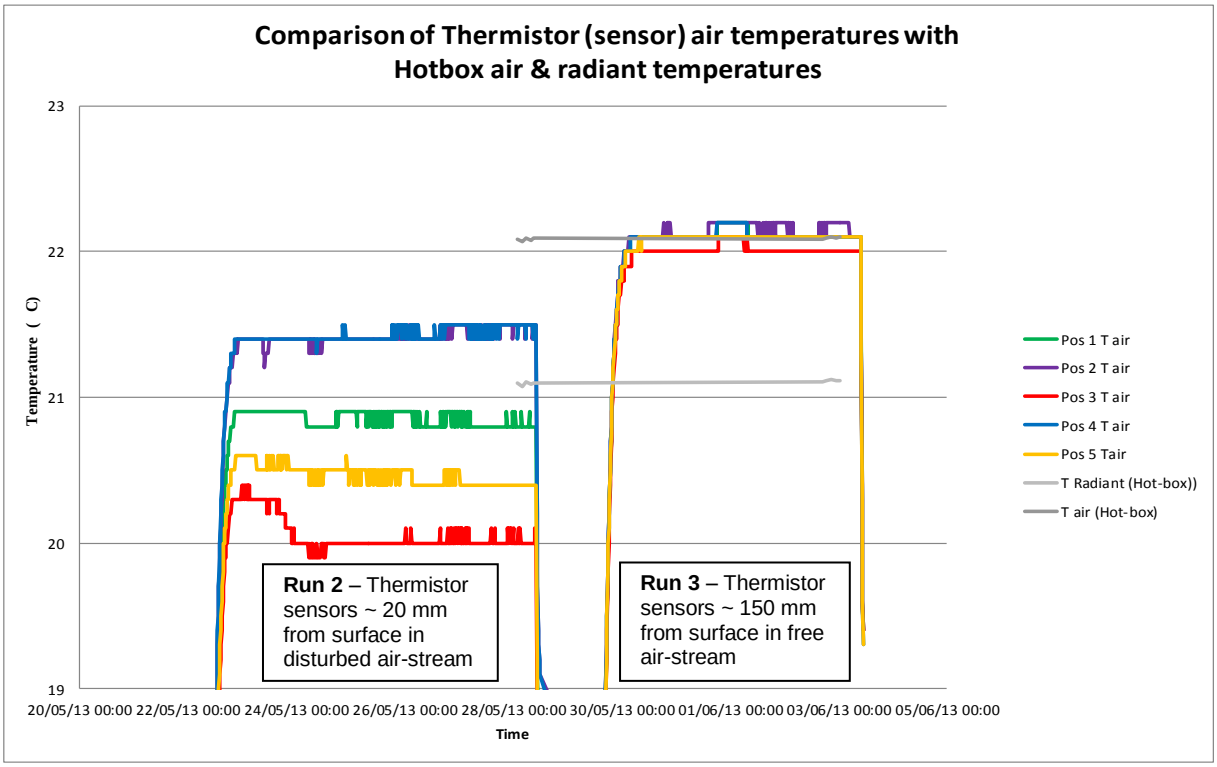

Figure 12 - Variation in air temperature close to the test-panel surface as measured by the thermistor sensors

The implication for the use of these sensors in situ is that there may be some instances where the air temperature and the radiant temperatures at the HFP location are sufficiently different that a small error might arise when the temperature being measured with the thermistor sensor is the air temperature and not the more correct environmental temperature (approximately 50% air temperature and 50% radiant temperature). The size of the error depends therefore on the difference between the air temperature and the mean radiant temperature. In most situations the air and mean radiant temperatures 'seen' by the HFP will be similar. However, if there is a nearby 'hot' radiant source, such as a wet radiator, or a nearby cold radiant sink, such as the surface of external glazing, the error being made by using air rather than environmental temperature may become more important[2].

2.3.2.4 Adjustment of the heat flux measured by the heat flux plates

Using the array of nine equally-spaced surface temperatures (both on the hot side and the cold side of the test panel), the surface temperatures close to the particular HFP were determined from suitable weighting. This was used with the known thermal conductance of the test panel to calculate the local heat flux adjacent to each HFP.

In general the heat flux, Φ, through a plane element is determined from the U-value of the plane element multiplied by the difference in environmental temperature across it, i.e.:-

$$\Phi = U \times (T_{\text{hot}} - T_{\text{cold}}) \qquad (1)$$

Both the heat flux plates and normal wall surfaces are considered to have the same high emissivity of around 0.9 and it is therefore reasonable to assume that the hot-side surface of the HFP experiences the same (but unknown) environmental temperature (T_{hot}) as experienced by the adjacent surface without the HFP present. The systematic error, S_{error}, that arises from using the HFP is then:-

$$S_{\text{error}} = \frac{\Phi_{\text{HFP}}}{\Phi_{\text{TP}}} - 1 \qquad (2)$$

where Φ_{HFP} is the heat flux measured by the heat flux plate and Φ_{TP} is the undisturbed heat flux adjacent to heat flux plate.

Figure 13 shows plots of the systematic error determined from equation (2) for each of the HFPs in all runs (from Run 2 through to Run 5) carried out on the test panel. Runs 2 and 3 have the HFPs pressure fixed to the plasterboard surface and Runs 4 & 5 have the HFPs pressure-fixed to the wallpaper surface with the embossed pattern. The odd numbered runs have the position of four of the HFP rotated (moved) as follows P1 to P2, P2 to P4, P4 to P5, P5 to P1 with P3 remaining undisturbed (i.e. not renewed as a pressure fixing). The starting positions of the HFPs in Runs 2 and 4 are the same, i.e. the same HFP is in the same starting position on both the plasterboard run and the wallpaper run. Table 3 shows the location of each of the HFPs during each run. The data points in the top and bottom plots are the same. The left-hand data points are in the run prior to rotation and the right hand data points are in the run after rotation. In the top two plots (left and right) the data points are linked to the same position being measured and in the lower plots (left and right) the link is to the same HFP. Position 3 (and HFP 6299) is

[2] For the on-going in situ measurements, some measurements will be made with additional temperature sensors that will enable any difference between air and radiant temperature to be determined. This will then allow the correct environmental temperature to be determined and used in the determination of the in situ U-value. In all cases any nearby radiant sources (or sinks) will be noted.

the unmoved and undisturbed HFP. Thus in the top and bottom plots we have the same two data points being linked.

Table 3: Location of individual HFP01 Heat flux Plates

	Run	P1	P2	P3	P4	P5
Plasterboard	**2**	**6218**	**6128**	**6299**	**6313**	**6217**
	3	**6217**	**6218**	**6299**	**6128**	**6313**
Wallpaper	**4**	**6218**	**6128**	**6299**	**6313**	**6217**
	5	**6217**	**6218**	**6299**	**6128**	**6313**

Considering the plasterboard surface (top left hand plot) and the unmoved HFP (green line), the systematic error is constant (hence a horizontal line). This is what is expected if the HFP and location are behaving consistently. For this particular HFP the systematic error is around -7%. By contrast, for the wallpaper (embossed) surface (top right plot), the systematic error for the unmoved HFP (green line) is not as constant between runs. In the first run the systematic error is about -11% and in the second it is just less than -5%. Also the *variation in systematic error* (as defined) for all HFPs is greater for the first wallpaper run compared to the second. It is not clear why that should be. One possible explanation is that the first wallpaper run was carried out only a day or so after the wallpapering of the test-panel (when the wallpaper may not have fully dried out and stabilised, whereas the second run would have been several days later when the wallpaper had more fully dried out.

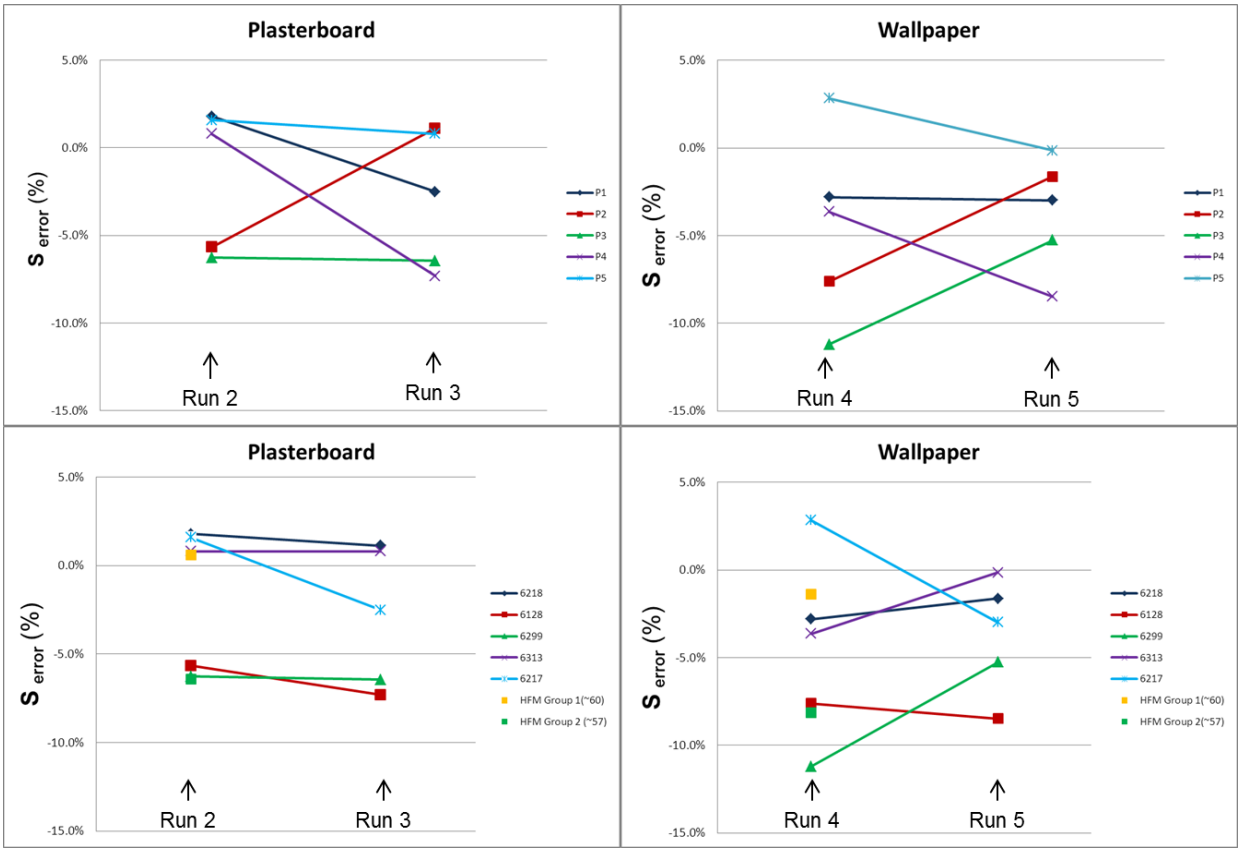

Figure 13 - Plots of the systematic error (as a percentage) between the heat flux as measured by the HFP and that measured by the Hot-box

Considering now the systematic errors for the moved HFPs and comparing with the values where the same HFP is measuring a different position, generally there is more consistency in the systematic errors for the same HFP (lower plot) than for the same position measured by a different HFP (top plot), indicated by the linked data points in the lower plot having lines of reduced slope (i.e. more horizontal) compared to the steeper slopes of the linked data points in the upper plots. This indicates that there is greater consistency in the systematic error for the same HFP and that the change of position has little effect on the behaviour of the HFP when moved and re-installed. An interesting and unexpected observation is that the level of systematic error for the five HFPs appears to group according to the magnitude of their calibration co-efficient.

Heat flux plates 6218, 6313 and 6217 form one group, where the calibration constant is near to 60μV/(W/m²) and the average systematic error is about +1%, and heat flux plates 6299 and 6128 with calibration constants of about 57μV/(W/m²) form the other group, which has a significantly negative systematic error of about -7%. It should of course be remembered that this variation of +1% to -7% (i.e. a range of 8%) in the systematic error is within the inaccuracy of the Hukseflux calibration system of ±5%, hence there is no reason not to use the average behaviour of the HFP (with their positional changes) when determining the systematic error from the hot-box runs. Table 4 summarises the various systematic errors that have been determined from these hot-box tests on the test panel. The average systematic error for the heat flux plates on the plasterboard surface is -3.8% and the mean range in values between initial run and run with the heat flux plates moved is ±0.7%. For the HFP on the embossed wallpaper surface, the average systematic error is larger, at -5.7%, but with an increased range in mean values of ±1.7%.

Table 4: Summary of the systematic error of the HFP from the hot-box tests

HFP Identifier	**Calibration. Co-efficient (μV/(W/m²)**	**HFP Surface**	**S_{error} (%)**	
			Mean	Range (+/-)
6218	60.70	Plasterboard	-0.2%	0.3%
		Wallpaper	-3.8%	0.6%
6128	58.11	Plasterboard	-8.0%	0.8%
		Wallpaper	-9.6%	0.4%
6299	58.58	Plasterboard	-7.9%	0.1%
		Wallpaper	-9.8%	2.9%
6313	60.56	Plasterboard	-0.9%	0.0%
		Wallpaper	-3.5%	1.7%
6217	61.13	Plasterboard	-2.1%	2.0%
		Wallpaper	-1.7%	2.9%
Plasterboard Average:			-3.8%	0.7%
Wallpaper Average:			-5.7%	1.7%

2.4 Thermal Modelling of calibration and in situ set-ups of heat flux plate

The magnitude of any systematic error that might arise from any differences between the HFP01 heat flux plate operating under its calibration set-up and the set-up used in the NPL Hot-box tests and in situ can

be determined theoretically from thermal modelling[3] of these different set-ups. The theoretical result can then be compared to the systematic error determined from the measurements made in the hot-box tests. It should be remembered that these models are steady state models and there may be some aspects of the calibration and in situ set-ups affected (to some extent) by non-steady-state influences. That said; the steady state models of these set-ups should be adequate in providing a reasonable estimate of the expected systematic errors that might arise.

2.4.1 Physical characteristics of the HFP01 sensor and its incorporation into the thermal models

The physical make-up of the HFP01 sensor is shown in Figure 14. All of these items are included specifically in the modelling of the HFP01, including the four air-space segments between the vertical edges of the active sensor and the sides of the 'hole' in the ceramic disc of the HFP01 (see Figure 15). Details of the materials making up the HFP01, their dimensions and thermal conductivities, are given in Table 5.

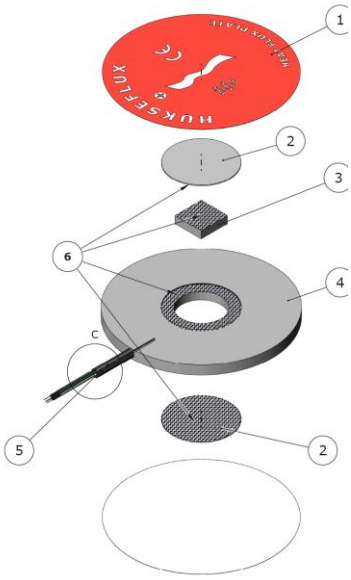

Figure 14 - Exploded view of the HFP01 heat flux showing its physical make-up

Item	Description
1	Red plastic label on the top (hot-side) of the HFP01. There is a similar (blue) plastic label on the reverse (cold-side) of the HFP01
2	Aluminium disc
3	Rectangular (active) sensor element. This fits in the circular 'hole' in the ceramic disc of the HFP01
4	Ceramic disc with recess for the thin aluminium disc that is put in place after (3) is inserted
5	Electrical leads that connect to the active element
6	Exploded view of two of item (2) and item (3) showing where they fit in the HFP01

[3] The thermal modelling was carried out using TRISCO software by Physibel, which complies with the validation procedures and examples given in BS EN ISO 10211:2007

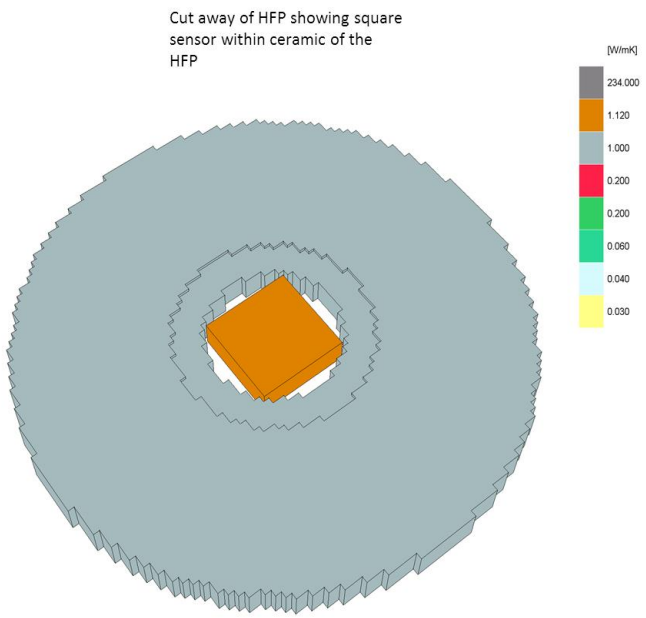

Figure 15 - Cut away image from modelled HFP showing active sensor and air gaps[4]

Table 5: Dimensions and thermal properties of the HFP01

Description	Diameter (Square) (mm)	Thickness (mm)	Thermal conductivity (W/m·K)
Plastic label (two)	79.0	0.1	0.20
Aluminium disc (two)	31.8	0.5	234.0
Rectangular (active) sensor element. This fits in the circular 'hole' in the ceramic disc of the HFP01	(14.8 x 14.8)	4.0	1.11
Ceramic disc with recess for the thin aluminium disc that is put in place after (3) is inserted	79.0	5.0	1.00
Air-space 'segments' (four)	-	-	0.028

[4] The circular cross-section of the HFP can only be approximated when using software which uses rectangular co-ordinates to define the geometry of the model. However, provided the 'step' size is sufficiently refined the errors will be negligible. The 'step' size used in these models is considered to be sufficient.

Figure 16 - Hukseflux Calibration apparatus showing locations for up to five HFP to be calibrated

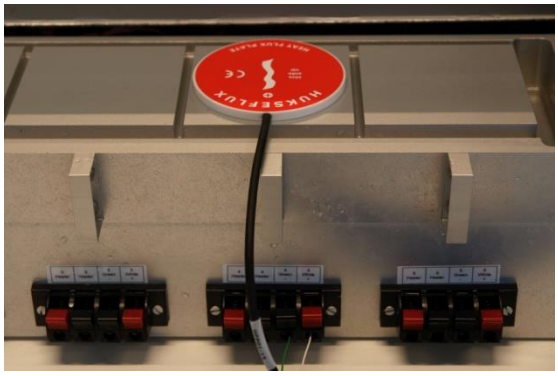

Figure 17 - HFP located on aluminium heat sink

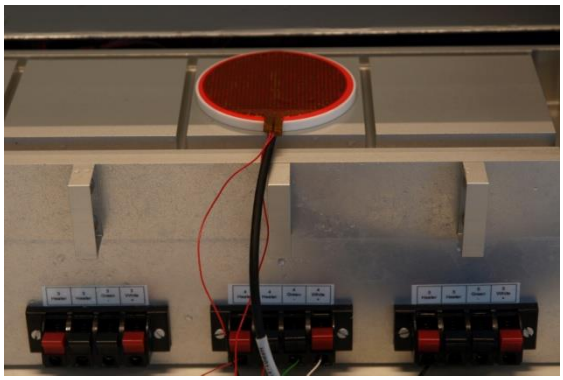

Figure 18 - Thin circular heater element on top of HFP

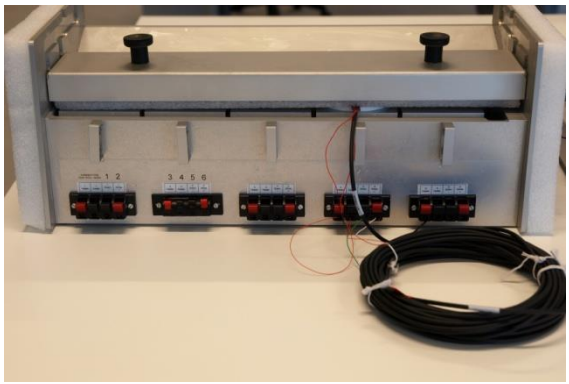

Figure 19 - Calibration apparatus with insulated lid closed over HFP

2.4.2 Calibration set-up of the HFP01 sensor

The Hukseflux HFP01 heat flux plate undergoing calibration is placed in the Hukseflux HFPC calibration apparatus. This involves the HFP being placed on an aluminium heat sink, whose temperature (for the duration of the calibration run) is considered to be constant at about 20ºC (the temperature of the laboratory). A thin circular heater element (70 mm diameter) is then placed on top of the HFP01. Approximately 1.1 W of power is delivered to the heater element. The lid of the calibration apparatus is insulated and it is estimated (by Hukseflux) that 99%[5] of the heat supplied will flow down through the HFP01. Figure 16, Figure 17, Figure 18 and Figure 19 show the calibration apparatus and the installation of the HFP in readiness for calibration. Glycerol is used between interfaces to ensure good thermal contact during calibration.

[5] The thermal modelling confirms this estimate with a calculated downwards heat flux which corresponds to 98.8% of the total heat input to the heater plate.

Figure 20 shows the heat flux out of the lid of the apparatus (left-hand image) and that down through the HFP and into the aluminium heat-sink (right-hand image). The heat is supplied to the heater plate for a short time (about 3 minutes) and the developed voltage of the sensor is recorded together with the power to the heater element. From these two quantities the calibration constant is simply the signal voltage from the heat flux plate divided by the downwards heat flux (in W/m²) into the HFP01 heat flux plate.

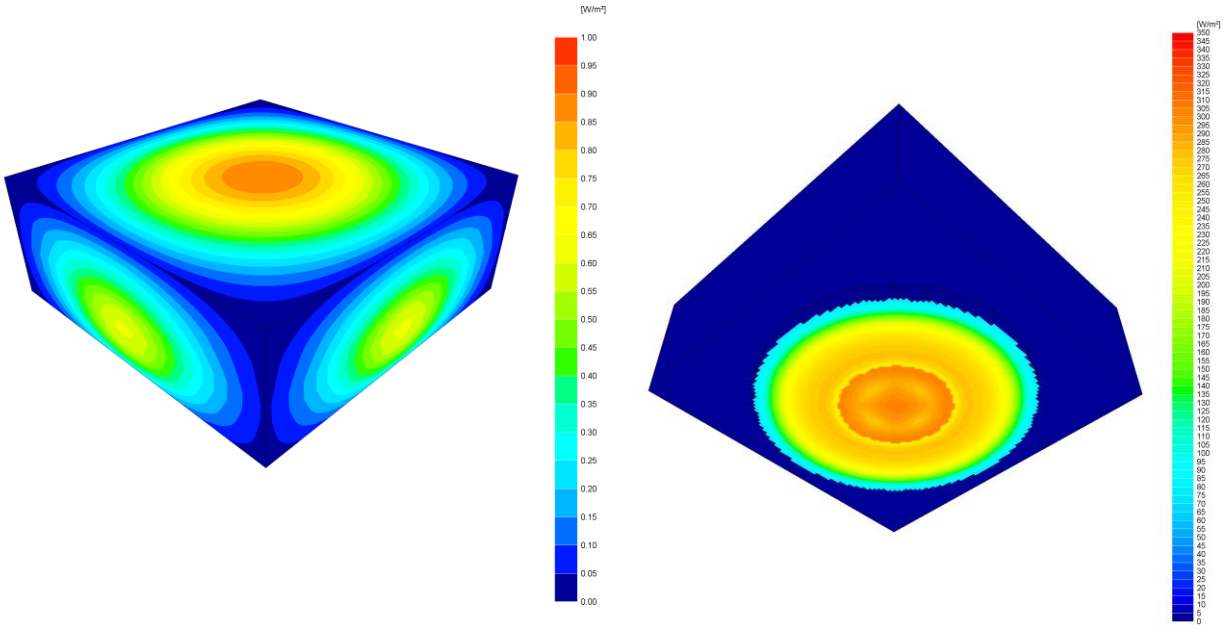

Figure 20 - Image showing heat flux out of the insulated lid (left-hand image) and the heat flowing out of the HFP and down into the aluminium heat-sink (right-hand image)

The HFP01 has a square active part (14.8 x 14.8 mm) and it is the temperature difference across this active part of the sensor that develops the signal voltage of the sensor. This temperature difference across the active part of the sensor is directly proportional to the heat flux through it and hence the developed voltage is also directly proportional to the heat flux through this active part of the sensor. If the thermal resistance across every region of the heat flux plate was constant then the heat flux across all regions would also be constant. However the physical make-up of the HFP gives rise to areas of different thermal resistance and hence varying heat-flux. This variation also gives rise to lateral heat flow components through and within the HFP. As a consequence, the heat-flux though the active area of the HFP01 is not the same as that through the HFP01 as a whole. The calibration constant is obtained from the total power that flows down through the heated area of the heat flux plate. This has a diameter of 70 mm compared to the overall diameter of the HFP of 80 mm and it is this slightly smaller area that is used in all the various thermal models when determining the heat flux through the HFP as a whole.

2.4.3 Hot-box and in situ set-up of the HFP01 sensor

The HFP pressure-fixed to the hot-side surface of the test panel in the hot box and those used in situ on a brick wall are very similar in their thermal behaviour. Figure 21 shows the heat flux through the HFP (pressure-fixed to the Test Panel) and that through the test panel itself and Figure 22 shows this for the HFP pressure-fixed to a solid brick wall. The images show clearly the reduction in heat flux (due to the presence of the HFP) together with the area around the edges of the HFP, where the heat flux continues to be disturbed.

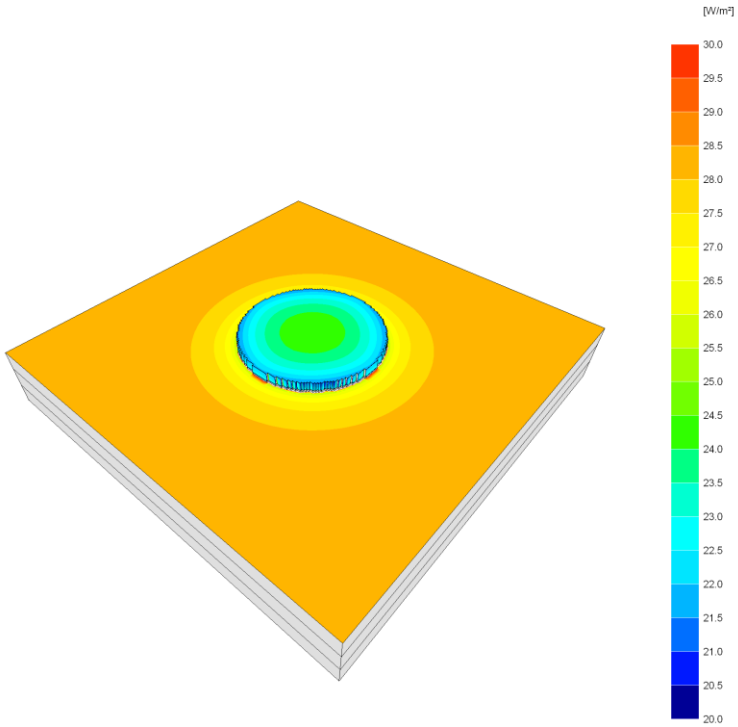

Figure 21 - Image of the heat flux through the HFP and the Test Panel

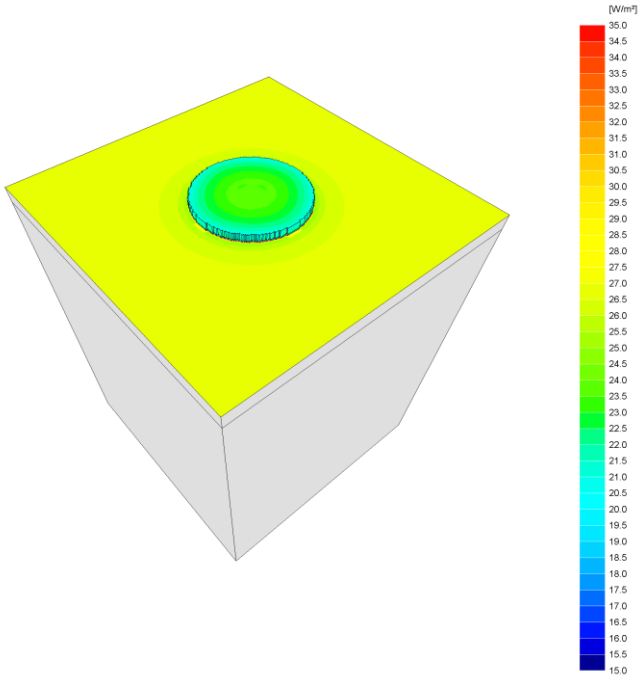

Figure 22 - Image of the heat flux through the HFP and the Brick wall

There is some lateral heat flow component to the heat flow through the HFP. What is required is the mean heat flux across the thickness of the HFP in order to compare this to the undisturbed heat flux through the test panel and so obtain the systematic error (as determined from thermal modelling). This systematic error comprises two elements. The first is a larger systematic error ($S_{1\ error}$) that arises from the heat flux through the HFP (when it is mounted on the test panel) being less than that through the test panel or in situ solid brick wall, without the HFP present, which is in fact the flux that we wish to determine from the HFP measurements. The second is a smaller systematic error ($S_{2\ error}$) that arises from the variation in heat flux through the HFP being slightly different between the calibration set-up and the in situ set-up.

2.4.4 Heat flux through the HFP01 sensor from the modelled calibration, hot-box and in situ set-ups

If the variation of heat flux across the HFP in use (e.g. when mounted on the surface of a wall) were identical to that under calibration, then there would be no smaller systematic error ($S_{2\ error}$) introduced to the measured heat flow (when using the calibration constant supplied). However, this is unlikely to be the case and, in order to determine the magnitude of this particular systematic error and the larger systematic error that arises from the HFP disturbing the heat flux (Φ), that is being measured, the heat flux through the HFP01 under calibration and in situ needs to be examined in more detail.

Figure 23 shows the heat flux through the hot and cold sides of the HFP01 heat flux plate. These heat flux distributions entering the hot-side and leaving the cold-side of the HFP are not identical; indicating that there is a degree of lateral heat flux within the HFP. The average heat flux distribution is determined from the mean of the heat flux through the hot and cold sides of the HFP sensor and it is this distribution of heat flux that is then compared with the in situ set-up of the heat flux plate, both in the hot-box test panel and on the internal surface of solid walls measured in situ.

These images of the heat flux distributions show clearly the underlying and identifiable structure of the HFP (as modelled).

The heat flux (both hot-side and cold-side) has been determined for four identifiable areas of the HFP as follows:

Area A_s is the area of heat flux through the rectangular active element of the HFP

Area A_1 is the area of heat flux through the four 'air-space' segments between the active sensor and the ceramic of the HFP

Area A_2 is the area of heat flux (R1 to R2) up to the edge of the aluminium of the HFP and

Area A_3 is the area of heat flux (R2 to R3) through the remaining ceramic of the HFP.

The total (mean) heat flux (hot-side and cold side) of the HFP as a whole is then determined from the area weighted averages of these four heat fluxes. The ratio of the heat flux Φ_s (through the active area A_s) to the total (mean) heat flux Φ_T (through the HFP as a whole) has been determined. The heat flux through the HFP in the set-ups of the HFPs in the hot-box test panel and of the HFP on the internal surface of an exposed solid wall show very similar distributions of the heat flux. Appendix B shows these heat flux distributions (through the HPF01 heat flux plate) and their detailed calculation for the calibration, test-panel and in situ solid wall set-ups.

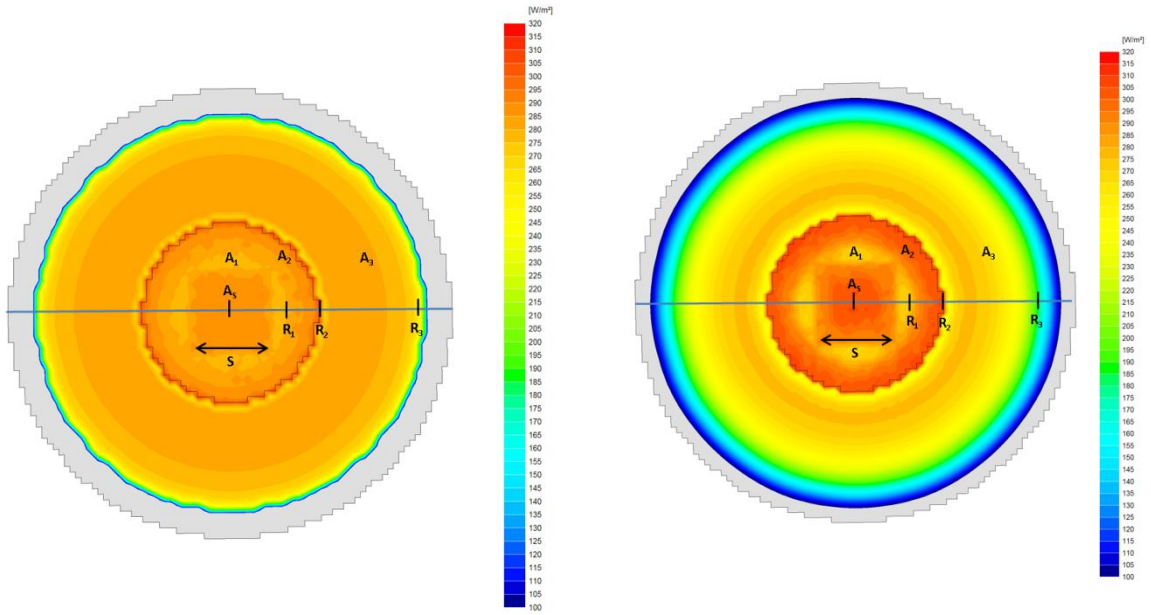

Figure 23 - Images of the heat flux through the hot-side (left image) and cold-side (right image) of the modelled HFP under the calibration set-up

The larger systematic error (determined from the thermal modelling) that arises from the presence of the HFP disturbing the heat flux, Φ, we are interested in is obtained from:

$$S_{1\,\text{error}} = \frac{\Phi_{\text{T(in-situ)}}}{\Phi_{\text{(undisturbed)}}} - 1 \qquad (3)$$

The smaller systematic error (determined from the thermal modelling) is obtained from:

$$S_{2\,\text{error}} = 1 - \frac{\Phi_{\text{S(cal.)}} / \Phi_{\text{T(cal.)}}}{\Phi_{\text{S(in-situ)}} / \Phi_{\text{T(in-situ)}}} \qquad (4)$$

The total systematic error from the modelling is then:

$$S_{\text{error}} = S_{1\,\text{error}} + S_{2\,\text{error}} \qquad (5)$$

bre

2.4.4.1 Results of the determined systematic errors provided by the thermal models

In the case of the NPL test panel, the systematic error; S_{error}, as determined from the thermal modelling is -8.0%, which compares to the measured systematic error (on a plasterboard surface) in the NPL hot-box of -3.8%. Considering the modelled result to be from a 'perfect' model (with all input data having no error), the difference of -4.2% in the systematic error of -8.0% (determined from thermal modelling of the HFP pressure fixed to the test panel) and -3.8% (determined from the various hot-box measurements on the plasterboard test panel), is well within the calibration uncertainty of the HFP ±5% and the ±5.5% uncertainty in the hot-box measured U-values or thermal conductance. Thus the systematic error implied from the hot-box measurements and that determined from thermal modelling of the HFP pressure-fixed to the test panel, are in good agreement.

The systematic error from the thermal modelling of a solid brick wall plus pressure fixed HFP is -7.4%, which compares to the -8.0% from the test panel plus HFP. This small difference in systematic error of about - 0.5% indicates that hot-box measurements on a solid brick wall with HFP pressure fixed to the test wall in the hot-box are likely to produce similar results to those investigated here for the hot-box test panel.

2.4.4.2 Sensitivity of the systematic error to the U-value of the wall being measured

The systematic error described in 2.4.4.1 has been determined for a specific U-value of 1.41 W/m²K (i.e. the U-value of the Test Panel). In order to check the sensitivity of the systematic errors with the U-value of the wall undergoing measurements (using the HFP01 HFPs), further numerical modelling was carried out looking at the S_1 and S_2 errors that arise for a range of U-values. Five additional models (1 to 5 in Table 6) were created to represent the full range of expected in situ wall U-values measured from uninsulated solid walls and uninsulated cavity walls to filled cavity walls and externally insulated solid walls. Table 6 gives the U-value of each model, the S_1 error (arising from the presence of the HFP), the S_2 error (arising from the calibration and in situ set-ups), the total systematic error S_{tot}, together with the 'apparent' thermal resistance of the HFP, R_{HFP}. The various values from the modelling of the test panel are included for comparison.

Table 6: Sensitivity of Systematic error with U-value

Modelled wall	U_{wall} (W/m²K)	R_{HFM} (m²K/W)	S_1 (%)	S_2 (%)	S_{tot} (%)
1	1.824	0.028	-4.9	0.2	-4.7
2	1.575	0.023	-3.4	-1.9	-5.4
3	0.961	0.042	-3.9	-1.5	-4.2
4	0.308	0.108	-3.2	-0.9	-4.4
5	0.287	0.150	-4.1	-0.3	-5.4
		Average:	-3.9	-0.9	-4.8
Test Panel	1.42	0.073	-6.7	-0.8	-7.5

R_{HFP} is obtained by expressing the S_1 error for the particular wall (and its U-value) as an implied additional resistance to that of the modelled wall, in order to achieve the systematic reduction in heat-flux as determined from the numerical modelling. The S_1 error for the test panel is a little higher compared to those for the solid wall. This is mostly a consequence of the surface being plasterboard instead of plaster. The S_2 error for the test panel is very similar to those from the solid plastered walls.

Various plots of the systematic errors (plus a plot of R_{HFP}) against the variation in U-value are shown in Figure 24

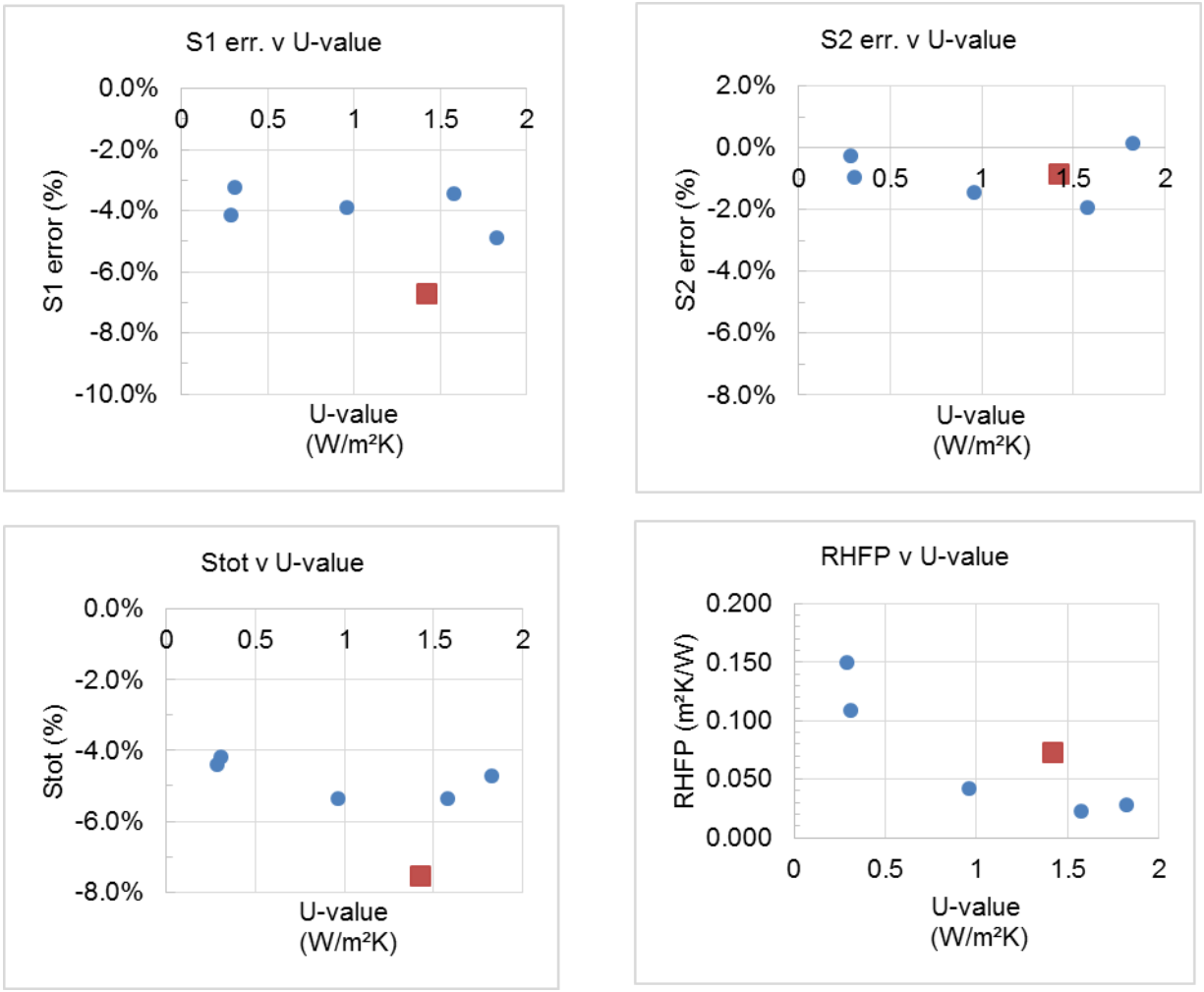

Figure 24: Plots of the sensitivity of the systematic error with U-value

One approach to correcting the measured heat flux is to consider that the presence of the HFP adds a fixed and constant thermal resistance to the building element undergoing the U-value measurement, irrespective of the U-value being measured. However, from the plot of R_{HFP} with U-value, the thermal modelling of the HFP on different walls with different U-values shows that the 'apparent' thermal resistance, R_{HFP}, of the HFP is not constant with the U-value of the wall being measured and thus the approach of simply correcting the measured U-value (by subtracting a constant R_{HFP}) is not adequate.

Looking at the remaining plots in Figure 24, the plot of the S_1 error (arising from the presence of the HFP) is reasonably constant varying from -3.2% to -4.9% with an average value of -3.9%. The smaller S_2 error is also reasonably constant varying from about 0.2% to -1.9% with an average of -0.9%. The total error (S_1 + S_2) varies from -4.2% to -5.4% with an average of – 4.8%. Consequently, an average total

systematic error correction can thus be applied to the measured heat flux and hence measured U-value, irrespective of the U-value of the wall being measured. Also, if this systematic error correction is applied regardless of a particular surface being plasterboard, rather than dense plaster this would introduce only a small error of 2 or 3% to the particular measurement, and since the vast majority of the in situ measurements (90%) are on solid walls with a dense plaster internal finish, the effect on the overall measurement statistics of applying this correction, irrespective of dense plaster or plasterboard surface, will be negligible. We can, therefore, conclude that it is reasonable to apply a total systematic error correction ($S_1 + S_2$) of approximately +5%. This equates to multiplying the initial measured heat flux (or U-value) by 1.05.

2.5 Steady-state compared to dynamic U-value measurements

As part of the overall Solid Wall Insulation project, a number of solid brick walls were built in the laboratory and installed for testing in a separate NPL hot-box, These walls are described in the report on this project "Understanding the thermal perfromance of solid walls" . The tests carried out were mostly steady-state, however one built-wall, Wall 3, also underwent some dynamic assessment in order to confirm (or not) that U-value measurements carried out under steady-state conditions produced the same result when carried out under varying internal and external temperature conditions. The heat-fluxes (and hence measured U-values) are not determined from the hot-box measured heat-flux but from the heat-flux as measured by three HFP01 HFPs located near to the centre position on the hot-side wall surface. The typical steady-state and dynamic conditions for these runs in the hot-box are shown in Figure 25.

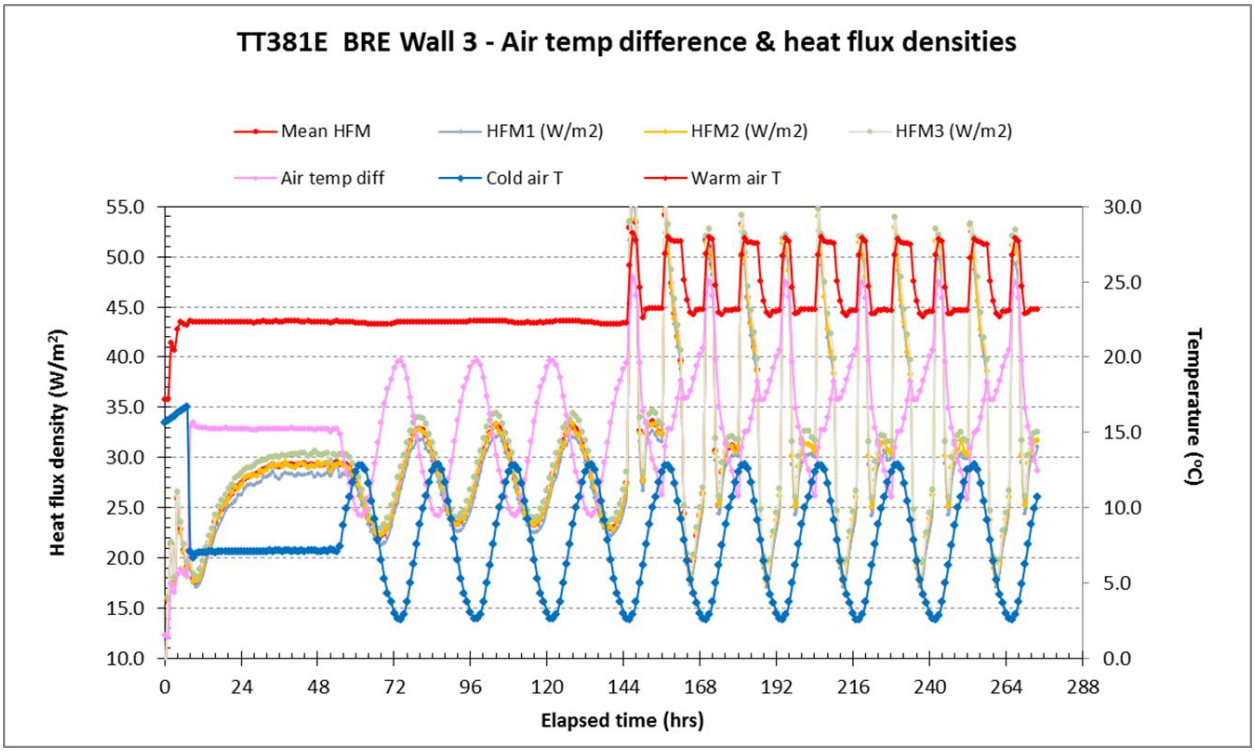

Figure 25: Steady-state and dynamic temperatures and measured heat flux from the HFP01 HFPs

The first main period shown in Figure 25, (following a brief set up period of a few hours which shows the creation of the intial conditions) runs up until approximatley 50 hours of elapsed time and represents the steady-state period with the hot-side air temperature (Warm air T) steady at about 22.5 °C and with the cold-side temperature steady at about 7.0 °C. The middle period, running between approximately 50 hours and 144 hours, has the warm-side temperature steady as previously but with the cold side temperature cycling between about 2.5 °C and 13 °C (this was to simulate the generality of the diurnal

external temperature). The last period, running from approximately 144 hours until the end of the test, shows the internal temperature controlled to simulate two heating periods – a shorter period in the morning and a longer one in the evening, where the hot-side temperature varied between 23.5 °C and 27.5 °C. Note that over the period of cold and hot-side temperature cycling the mean temperature of the wall has increased from about 14.5 °C to about 16.0 °C.

Figure 26 shows an extended period of hot-side and cold-side cycling temperatures (from elapsed time 168 hours onwards) and the resulting cumulative U-value for the uninsulated Wall 3. The cumulative U-value is determined from the sum of the average heat-flux (as measured by the three HFP) divided by the sum of the temperature difference over the relevant period of the test run.

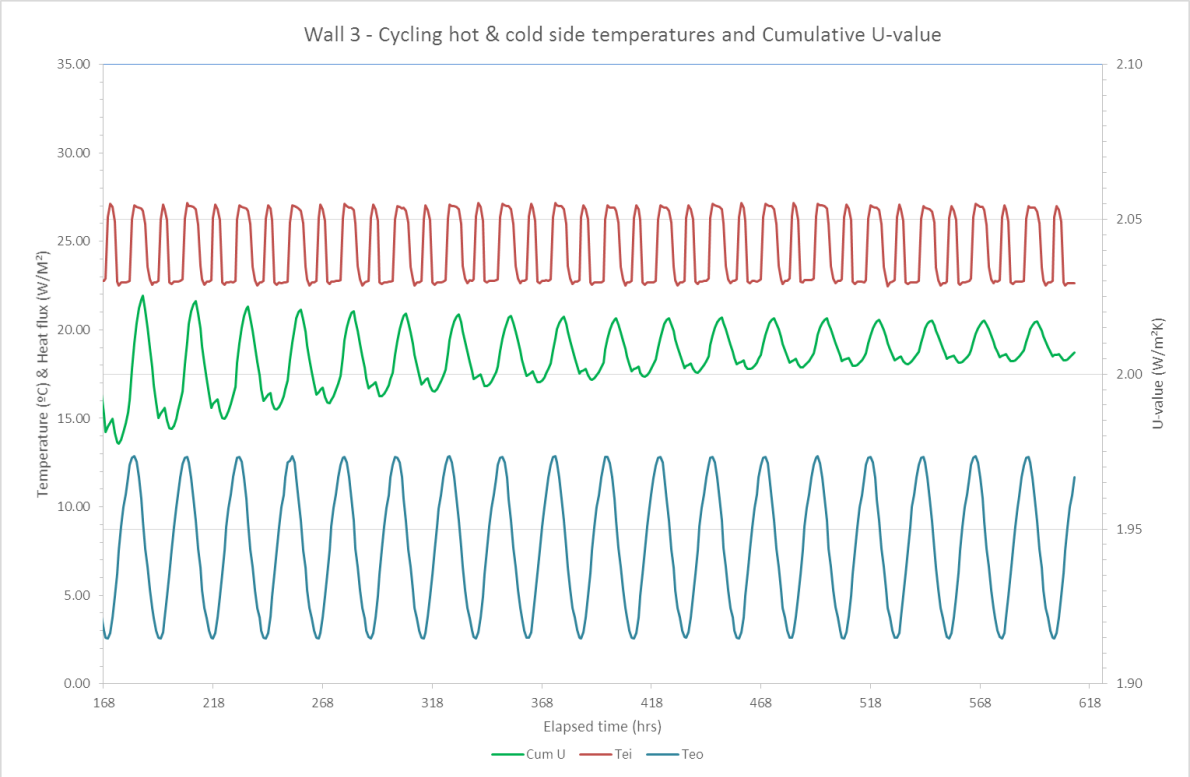

Figure 26: Wall 3 (uninsulated) – Hot-side and Cold-side temperature cycling and the resulting cumulative U-value as measured by the HFP01 HFPs.

Steady-state and cycling temperature runs were also carried out for Wall 3 with external insulation installed well (Insulation 1) and then with poorly installed external insulation (Insulation 2). Thus steady-state and 'dynamic' U-values were obtained for three conditions of Wall 3 – uninsulated, well insulated and poorly insulated. Table 7 summarises the steady-state and dynamic U-values that were obtained for these three variants of Wall 3.

For the uninsulated Wall 3 the steady-state U-value is 1.970 W/m²K and this compares to the dynamic U-value of 2.014 W/m²K. The change in U-value from Steady-state to Dynamic is + 2.2 %. For Wall 3 with well installed external insulation, the steady-state U-value is 0.315 W/m²K and this compares to the dynamic U-value of 0.320 W/m²K with a change in U-value from Steady-state to Dynamic of + 1.6 %. For Wall 3 with poorly installed external insulation, the steady-state U-value is 0.329 W/m²K and this compares to the dynamic U-value of 0.328 W/m²K with a change in U-value from Steady-state to Dynamic of – 0.0 %.

Table 7: Steady-state and Dynamic U-values for Wall 3 variants

Description	Steady-state U-value (W/m²K)	'Dynamic' U-value (W/m²K)	ΔU (Dynamic - Steady-state) (W/m²K)	Change in U-value
Wall 3 - Uninsulated	1.970	2.014	+ 0.044	+ 2.2%
Wall 3 – External insulation installed well	0.315	0.320	+ 0.005	+ 1.6%
Wall 3 – External insulation poorly installed	0.329	0.328	- 0.001	- 0.0%

Thus the variation in U-value measured under steady-state and under dynamic temperature conditions is approximately 2% or less. This error is small and well within the experimental error of these hot-box runs (estimated at ± 6.5%) but it should also be understood in the context of typical in situ U-value measurement errors using this type of HFP (namely the Hukseflux HFP01 HFPs) of around 15%. From a detailed inspection of the data from the various hot-box runs, there is some indication that for some runs, even with the very well controlled temperatures of the hot-box (both steady-state and dynamic cycling) the period of data for analysis, i.e. the duration of the hot-box runs, should have ideally been longer. With longer duration runs (steady-state and dynamic) it seems likely that these would have have produced even closer agreement between the steady-state and dynamic U-values being measured. Nevertheless, the conclusion is that measuring U-values in situ, under the usual variation in internal and external temperatures and using the HFP01 HFPs, produces a measured U-value that is representative of the underlying steady-state U-value that is a property of the construction being measured.

2.6 Tests 1 and 2 Conclusions

2.6.1 Thermistor (steel-tube) temperature sensors

It was found from the hot-box measurements that the polished steel-tube thermistor temperature sensors that are used in situ measure very close to air temperature. Thus there may be some historical in situ U-value measurements where the air temperature and the radiant temperature of surrounding surfaces are sufficiently different that a (probably) small error may result from measuring the air temperature instead of the more correct environmental temperature of 50% air temperature and 50% radiant temperature. This possibility is being investigated by this project with the use of additional temperature sensors in fieldwork.

2.6.2 Pressure-fixing of the HFP01 heat-flux sensor

The in situ pressure fixing system was duplicated in the hot-box runs and it was found that the HFP01 heat flux plate made good thermal contact with both a smooth plasterboard surface and an embossed wallpaper surface. After adjustments to take into account some minor temperature variations across the surface of the test panel, on average, the heat flux measured by the HFPs were, in the case of the plasterboard surface, 3.8% lower than that determined from the hot-box measurements and, in the case of the embossed wallpaper surface, 5.7% lower.

2.6.3 Validation of the in situ method of determining U-values using heat flux plates

The NPL hot-box measurements on the test panel (plasterboard surface and embossed wallpaper surface) and the thermal modelling of the HFP on the test panel, indicate a systematic error in the measured heat flows of between -3.8% (hot-box test panel, plasterboard surface) and -8.0% (from thermal modelling). The additional numerical modelling, which indicated that the systematic error correction was relatively constant with the U-value of the wall being measured, provided an average systematic error correction of +5%, where this can be applied to *all* measured heat fluxes and hence applied to *all* determined U-value measurements. In addition, it has been demonstrated from the comparison of steady-state and dynamic hot-box measurements that the HFP01 HFPs as used in situ, i.e. measuring under non steady-state internal and external temperature environments, measures a U-value that represents the underlying steady-state U-value, where this is a property of the bulding element being measured.

The overall conclusion from this series of hot-box tests and the thermal modelling of the calibration and in situ use of the HFP01 heat flux plates is that, within the accuracy of the hot-box measurements and HFP measurements, both the hot-box measured U-value and that measured by the HFPs are in agreement. Hence the use of the HFP01 HFPs as a method of measuring in situ U-values of building elements, such as a solid brick wall (uninsulated and insulated), is validated. Consequently, for all in situ U-value measurements where an HFP01 HFP is used, the measured U-values should be corrected by multiplying them by a correction factor of 1.05.

3 Test 3 – Reproducibility of the sensor substrate

3.1 Introduction to the field tests

The field tests (ie Test 3 to Test 7) were conducted in a vacant dwelling in West London between February and June 2014. The dwelling was a first floor flat in a semi-detached block and the front view of the dwelling is shown below. Owing to its unusual shape, it had exposed facades on all four sides, making it particularly suitable for these experiments. The north façade had a 1.5 or 2 brick thick wall with a thickness of around 13.5" while the other facades were 1 brick (i.e. 9 inches) thick. The east and west walls were relatively free of sunlight in the winter due to the urban location and proximity of other buildings. The walls were wallpapered however permission was granted by the owner for the wallpaper to be stripped because a major refurbishment was anticipated. The plan drawing in Figure 28 gives some idea of the configuration of the dwelling.

Figure 27 - Front view of dwelling

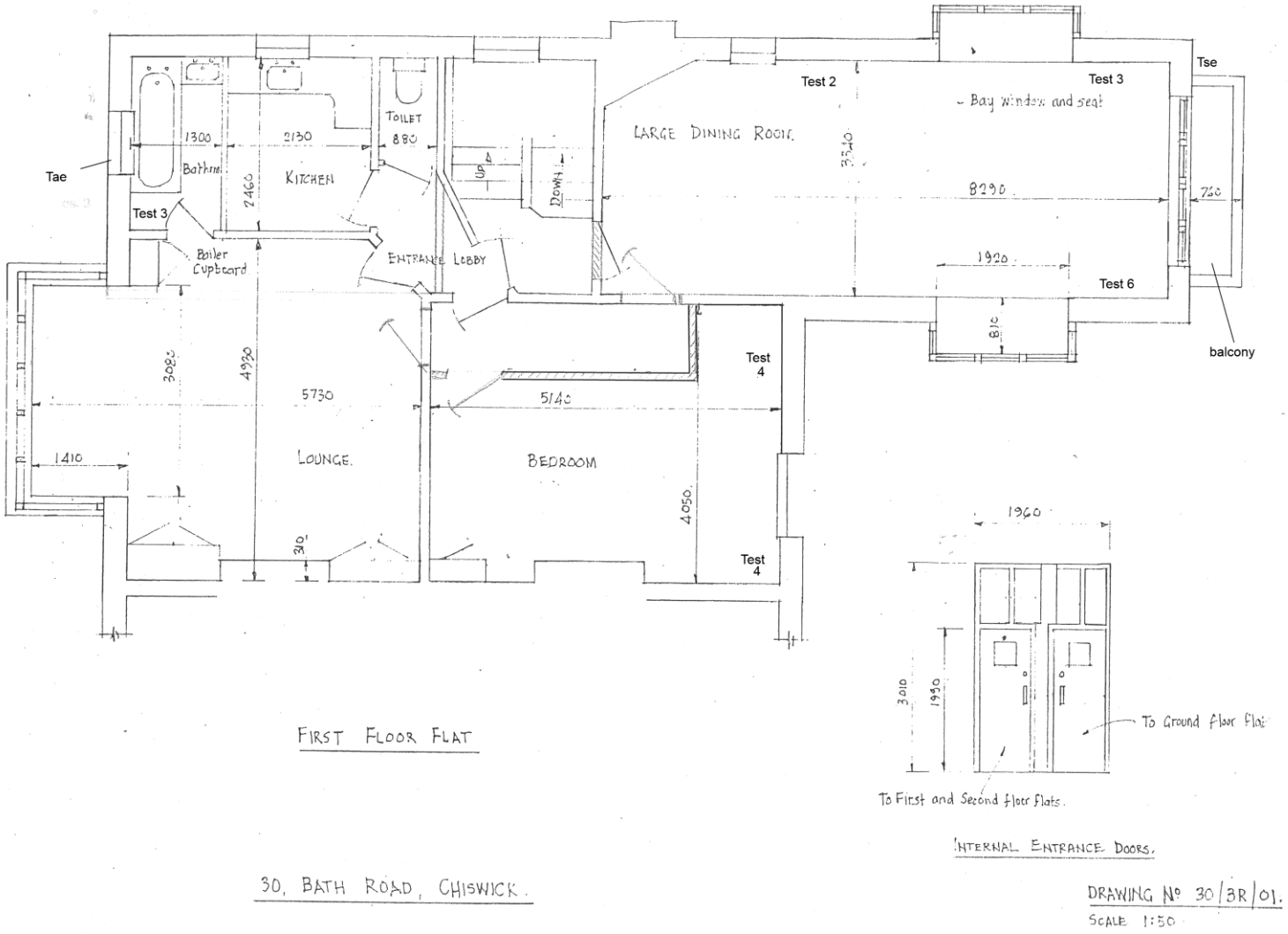

Figure 28 - Plan drawing of dwelling used for field tests (front façade to the left)

Internal temperature was controlled using the central heating system. Since the dwelling was vacant and had not been heated for some time, there was a possibility that the moisture content of the walls might be unusually high. In order to reduce this potential problem, the heating was switched on a few weeks before commencing the measurements. The heating was provided by a new gas combination boiler with radiators in all rooms. It was switched to continuous, and set at a relatively high temperature, in order to provide a good contrast in temperature with the outside air. The room thermostat for the property was located in the bedroom.

3.2 Test 3 results and conclusions

Test 3 examined the reproducibility of the thermal contact between a heat flux plate and the wall which it is being used to test.

The degree of thermal contact between a sensor and a wall can be influenced by the variation in the application of petroleum jelly and in the application of the cling film, as well as variations in the amount and size of air bubbles and variation in the way different people apply it. It might also be influenced by the pressure exerted by the flexible clamps that are used. This test was conducted through repeated heat flux measurements, at exactly the same locations, but with the substrate (Vaseline and cling film) renewed for most of the measurements.

In order to test the reproducibility of the method of applying a substrate, affixing heat flux plates and measuring U-values, the U-value at specific points on the east wall were repeatedly measured at eight locations. These positions, running from left (farthest north on the east wall) to right (farthest south on the east wall) were labelled 1A, 2A, 3A, 4A, 1B, 2B, 3B and 4B. For six of the plates (1A, 2A, 4A, 1B, 2B and 4B), the substrate was removed and re-applied. The two remaining plates (3A and 3B) retained the same location and substrate application throughout the entire measurement period in order to serve as a control group. The application of substrate was carried out by three different people so that human variation could be included within the overall variation. One person applied the Vaseline and Clingfilm on 25 February, a second person applied the Vaseline and Clingfilm on 7 March and a third person applied the Vaseline and Clingfilm on all of the subsequent visits.

Table 8 shows the key dates. Table 9 shows the heat flux levels recorded at each position.

Table 8 - Key dates for test 3

Period	Start date	End date	Tasks at beginning of period
-	07/02/14	25/02/14	Heating switched on
1	25/02/14	07/03/14	Monitoring equipment installed (by Person 1)
2	07/03/14	19/03/14	Substrate renewed at positions 1A, 2A, 4A, 1B, 2B and 4B, but not at 3A & 3B (by Person 2)
3	19/03/14	28/03/14	Substrate renewed at positions 1A, 2A, 4A, 1B, 2B and 4B, but not at 3A & 3B (by Person 3)
4	28/03/14	07/04/14	Substrate renewed at positions 1A, 2A, 4A, 1B, 2B and 4B, but not at 3A & 3B (by Person 3)
5	07/04/14	17/04/14	Substrate renewed at positions 1A, 2A, 4A, 1B, 2B and 4B, but not at 3A & 3B (by Person 3)
6	17/04/14	23/06/14	Substrate renewed at positions 1A, 2A, 4A, 1B, 2B and 4B, but not at 3A & 3B (by Person 3)
-	23/06/14	-	Equipment de-installed

Table 9 – Mean heat flux observed at each position (W/m^2)

Period	1A	2A	3A	4A	1B	2B	3B	4B	Average mean flux	std. dev. *
1	20.370	17.831	18.615	18.639	19.624	19.147	20.080	17.680	18.998	0.989
2	14.463	13.509	13.691	13.916	14.355	14.208	14.825	12.831	13.975	0.629
3	19.135	17.283	17.127	17.901	17.983	17.426	18.872	16.179	17.738	0.959
4	10.338	9.465	9.808	9.779	10.163	9.871	10.373	9.037	9.854	0.451
5	12.402	11.476	13.029	12.940	12.335	12.305	13.073	12.020	12.448	0.552
6	6.293	5.758	6.823	6.836	6.217	6.220	6.721	6.188	6.382	0.366

*This is the standard deviation in heat flux, to indicate the degree of spatial variation.

From inspection of Table 9, the following are concluded:

- The readings for positions 3A and 3B do not seem to differ significantly from the readings for the other positions. This suggests that re-application of the Vaseline and cling film does affect the measured heat flux (and therefore U-values) significantly.
- Running from the top to the bottom of the table, the measured heat fluxes generally fall as we move from winter, to spring, to summer; as would be expected.

Table 10 replicates the mean flux and standard deviation from Table 9 and presents the ratio of these. In addition, the column entitled 'T_{ai}-T_{ae}' indicates the mean difference in measured air temperature between inside and outside during the corresponding time period. The standard deviation in the heat flux, divided by the mean, has a relatively constant value, indicating a constant behaviour of the HFP measurement throughout the various periods of this test.

Table 10 - Mean temperature differences for each period

	mean flux (W/m^2)	**std. dev. (W/m^2)**	**std. dev / mean**	**T_{ai}-T_{ae} (K)**
period 1	18.998	0.989	0.052	13.350
period 2	13.975	0.629	0.045	10.222
period 3	17.738	0.959	0.054	13.366
period 4	9.854	0.451	0.046	7.375
period 5	12.448	0.552	0.044	9.908
period 6	6.382	0.366	0.057	6.661

It is worth noting that the measured heat flow does not vary significantly from one position to the next even though the substrate was replaced at some positions and not at others, indicating that re-application of the substrate to the HFP does not appear to change the heat flow significantly.

The conclusion from Test 3 is that the repeatability of the install of the HFP pressure-fix system is good and is not dependent upon the particular install or installer.

bre

4 Test 4 – Method of affixing the sensor

This test looks at the method of pressure-fixing. Pressure-fixing is preferable to adhesive in occupied housing because it avoids damaging internal finishes. The drawback is that the pressure-fixing method and the substrate to the HFP might distort the heat flow patterns, leading to inaccuracies in the measurement of the U-value. It also involves the use of tele-prop poles to provide an anchor point for the gutter clamps used to apply pressure to the HFP. These are more visually intrusive and could increase the risk that the apparatus could get knocked or disturbed by occupants (although steps are taken in occupied dwellings to minimise this risk). This test involved comparing the results obtained by pressure-fixing with those obtained by simply attaching the heat flux plates using adhesive tape.

These tests were conducted in two different locations within the flat. They were carried out on the east wall of the largest room and on the north wall of the bathroom. Some of the heat flux plates were pressure-fixed in the usual way, using tele-props and plastic gutter clamps, while other heat flux plates were affixed using adhesive tape. A total of eight HFPs were used.

The double-sided adhesive tape that was initially used proved to be ineffective. The plates generally fell off and corresponding gaps are seen in the data (indicated by low or zero heat flux readings). Alternative types of double-sided adhesive tape were tried on some of the later visits. Some of the heat flux plates were affixed using duct tape placed over the front of the plates. With this variation there was concern that the duct tape might have a different emissivity value from the heat flux plates themselves, leading to an error in the U-value measurements (a low emissivity would lead to a high internal surface resistance). Separately, the onset of spring and the reduction of the temperature contrast between inside and outside added to concerns about the accuracy of this test.

The HFPs used are shown in Figure 29 and the method of fixing are summarised in the table below.

Table 11 - Details of test 4 equipment setup

Position	**1A**	**2A**	**3A**	**4A**	**1B**	**2B**	**3B**	**4B**
HFP serial number	6250	6249	6202	6123	6303	6306	6256	6208
Fixing method	clamp	tape	clamp	tape	clamp	tape	clamp	tape
Façade	Side				Front			
Orientation of wall	East				North			
Room	Dining room				Bathroom			

The picture below shows the two fixing methods being tested. This shows the duct tape placed over the HFPs in positions 2A and 4A.

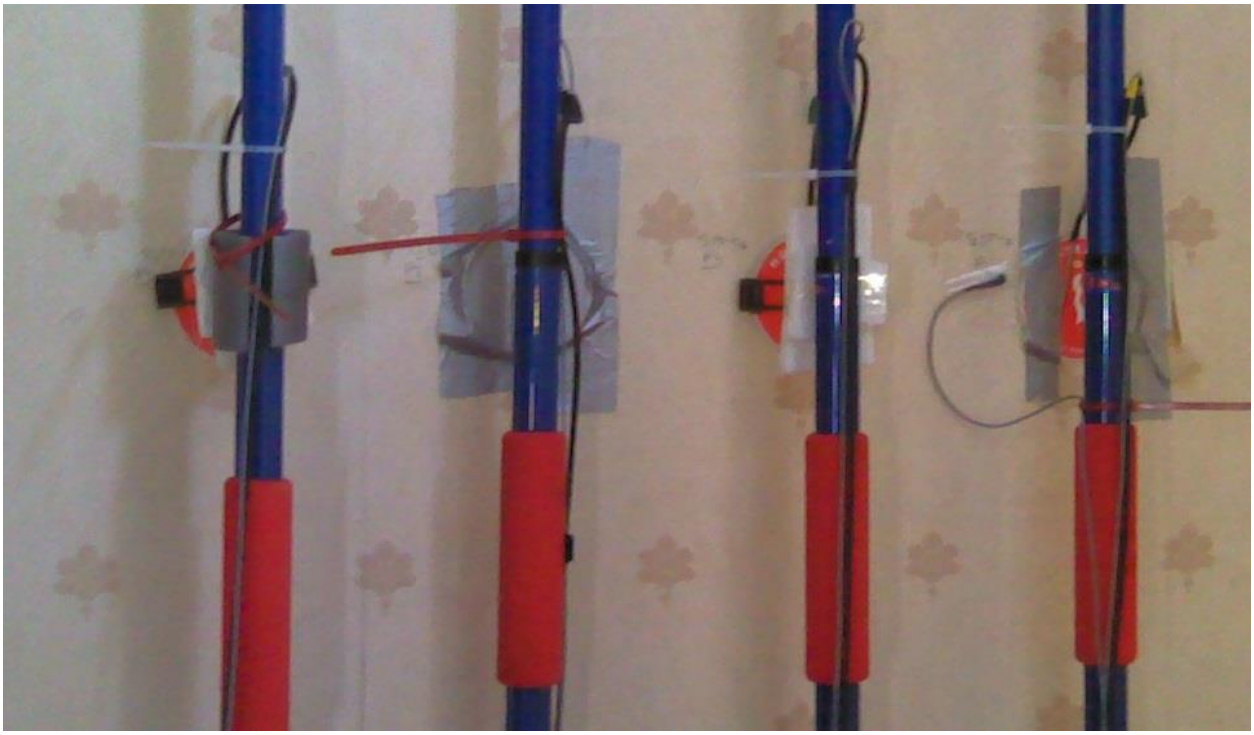

Figure 29 - HFP fixing methods setup. Positions are (from left to right) 1A, 2A, 3A and 4A

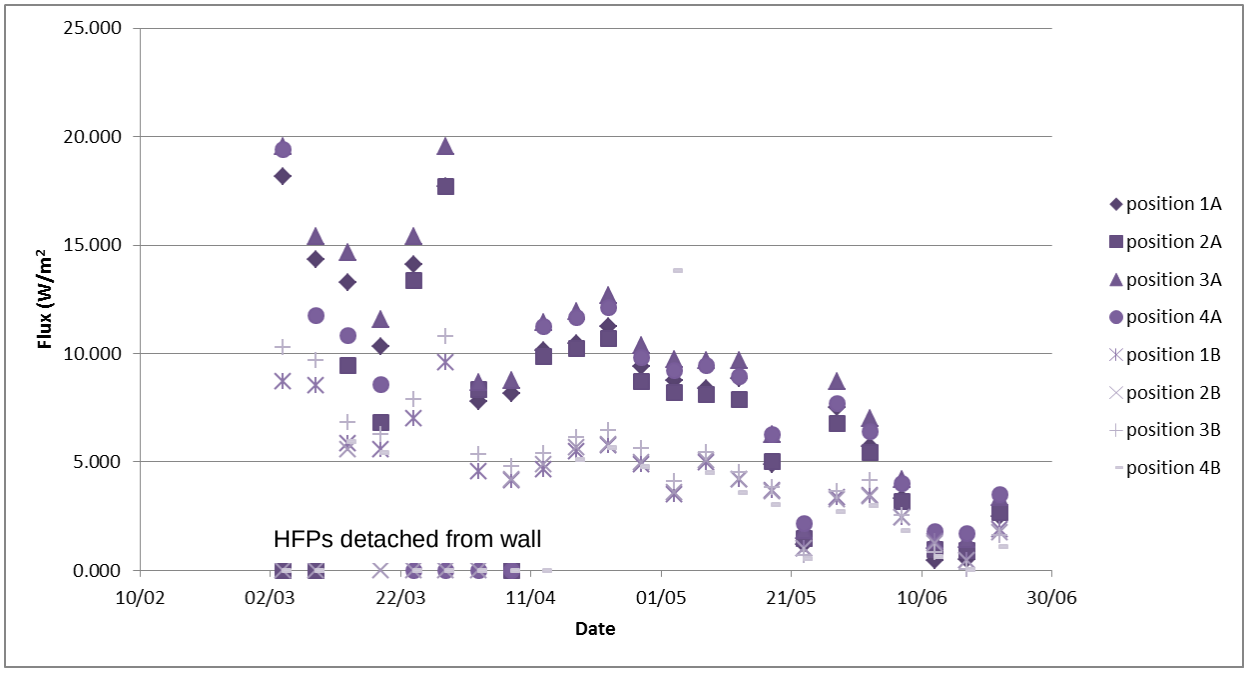

Figure 30 - Heat flux for each time period at each measurement location

Figure 30 shows the heat flux measured at each heat flux plate, versus time. As expected, there is a downward trend in the heat flowing into the wall as we move from winter into spring and through into summer. For some of the plates, the heat flux fell to zero; or close to zero, and it is noteworthy that these points corresponded to positions where tape was used rather than clamps. The heat fluxes in these cases were zero or close to zero because the plate had either fallen off or had become partially detached from the wall. The measured heat flux will be proportional to the apparent U-value which would result from the measurement, and the percentage reduction in the heat flux resulting from poor thermal contact is the same as the percentage reduction in the apparent U-value which would result from the partial or complete detachment of the sensor.

The heat fluxes presented above produce the U-values in the table below. It shows U-values for each 5-day period, for each of the eight measurement locations used in this test. The two columns to the extreme right show the mean and standard deviation of each U-value. The rows at the bottom of the table also show the mean and standard deviation.

Table 12 - U-values for each time period at each measurement location

Date	1A	2A	3A	4A	1B	2B	3B	4B	mean	std. dev.
03/03	1.352	-	1.519	1.482	0.777	-	0.912	-	1.088	0.729
08/03	1.310	-	1.479	1.079	0.995	-	1.121	-	0.967	0.665
13/03	1.231	0.869	1.373	1.020	0.801	0.727	0.933	0.832	1.123	0.223
18/03	1.051	0.685	1.184	0.880	0.940	-	1.054	0.935	0.950	0.216
23/03	1.169	1.079	1.288	-	0.750	-	0.839	-	0.884	0.596
mean	1.22	0.88	1.37	1.12	0.85	0.73	0.97	0.88		
std. dev.	0.12	0.20	0.14	0.26	0.11	-	0.11	0.07		

The hyphens in the table indicate that the U-values for those dates and locations are unreliable due to the heat flux plate being loose or detached from the surface of the wall. It is notable that the U-values are relatively steady during the earlier weeks but tend to decrease over time, perhaps due to the corresponding changes in external conditions – i.e. the onset of spring. The U-values were generally lower on the north wall than they were on the east wall, perhaps due to the north wall being thicker (~13.5” compared to ~9”).

During some visits, it was noted that although the heat flux plates affixed using tape were in contact with the wall, the contact between the heat flux plate and the wall was often partial and incomplete. This may have influenced the heat flux readings, leading to an underestimation of the U-value.

Inspection of the figures suggests that, during the colder weeks at least, the U-values tended to be slightly lower for the heat flux plates that were affixed using tape rather than by the usual pressure-fix method. The reasons for this are not clear, however the following are suggested:

- The low emissivity of the duct tape placed over the heat flux plate, leading to a higher surface thermal resistance, or

- Air pockets behind the heat flux plates.

The thermogram below shows the heat flux plates that were used for Test 3 on the east wall. It suggests that the tape might be reflecting some infrared radiation. A visible-light image is also shown for comparison. If the tape is generally reflective in infrared, this will tend to increase the surface resistance and therefore reduce the measured U-value.

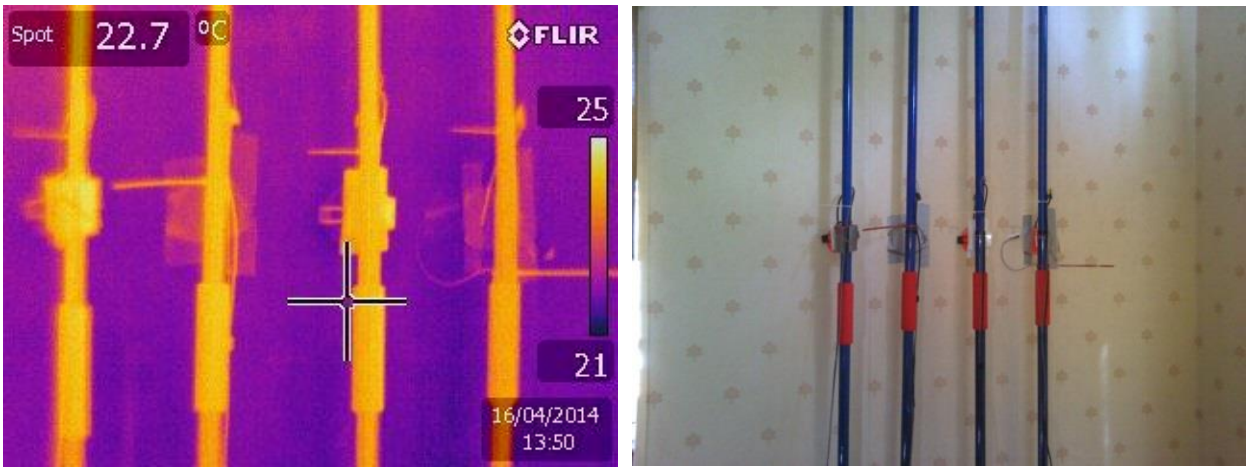

Figure 31 - Thermogram showing possible influence of duct tape

The results of this test are probably inconclusive due to the difficulties experienced when using double-sided tape to affix the heat flux plates to this type of wallpaper surface (old, poorly adhered wallpaper). If this test were to be repeated, it might be advisable to carry out the test on a more stable, painted surface, or at least one which would be more amenable to the use of double-sided adhesive tape (i.e. clean and free of dust).

In future studies it may be interesting to compare the pressure-fixing method of affixing heat flux plates with the adhesive based system used by Glasgow Caledonian University (Figure A2 of “Research into the thermal performance of traditional brick walls, research report 1, Paul Baker, Glasgow Caledonian University, 2013, prepared for English Heritage[2]) in order to put an upper limit on the possible disagreement between the two.

5 Test 5 – The influence of sunlight

This test looked at the impact of sunlight on the accuracy of U-value measurements. The impact of sunlight could be particularly important for south-facing facades and until now efforts have been made to avoid south-facing facades whenever possible (whenever testing occupied houses). This further restricts the available locations to conduct a U-value measurement and when other practical considerations are taken into account it can be hard to find any suitable locations in a dwelling. The test seeks to determine whether U-values can be measured on south facades and what effect doing so might have on the accuracy of the measurement.

This test involves continuous measurement of the U-value on a south-facing wall, with the intention of comparing the apparent U-value obtained on a sunny week with the apparent U-value obtained on a cloudy week. The drift in the U-value between sunny weeks and cloudy weeks should provide an indication of the impact of direct sunlight on the accuracy of the measurement. This test was carried out on the south wall of the bedroom.

Various external temperatures were measured (in different ways) and the results compared with a solarimeter. This was done to investigate options for detecting when the sun was shining and to see what effect this had on the various external temperatures as measured. The temperature sensors and methods used were:

- silvery sensor (T_s)
- sensor in mini Stevenson screen (T_{ss})
- black sensor, i.e. sensor covered by black tape (T_b)
- black sensor (as above) within glass vial (T_{bv})
- sensor on brick surface (T_{br})

The temperature of the black thermistor within a glass vial (T_{bv}) was compared with the temperature recorded by the silvery thermistor (T_s). A preliminary examination of the data quickly revealed that the black thermistor in the vial was generally warmer than the silver thermistor during the day, but at night the black thermistor in the vial was at a slightly lower temperature than the silvery thermistor. Figure 32 shows the setup of these two sensors.

Figure 32 - Silvery thermistor and black thermistor in a glass vial

A strong correlation was observed between $T_{bv} – T_s$ and the solarimeter readings. Table 13 shows that the temperatures measured by the silvery sensor and by the sensor in the Stevenson screen are very close. It also shows that the difference in temperature between the black sensor and the silvery sensor is a better indicator of sunlight (as compared to the solarimeter reading) when the black sensor is in the glass vial.

Table 13 - Degree of correlation of sunlight detection methods

First quantity	Second quantity	Correlation coefficient
Stevenson Screen temperature, T_{ss}	Temperature sensed by silvery sensor, T_s	0.995
Solarimeter reading in mV	$T_{bv} – T_s$ (T_{bv}, black sensor in vial)	0.91
Solarimeter reading in mV	$T_b – T_s$ (T_b, black sensor, no vial)	0.84

where T_{bv} was the temperature sensed by the black sensor within the vial, T_s was the temperature sensed by the silvery sensor and T_{ss} was the external temperature sensed by the Stevenson screen.

The following scatter plot (Figure 33) shows the data underlying the correlation between T_{bv}-T_s (the temperature of the black sensor in the vial and that of the silvery sensor) and the signal from the solarimeter.

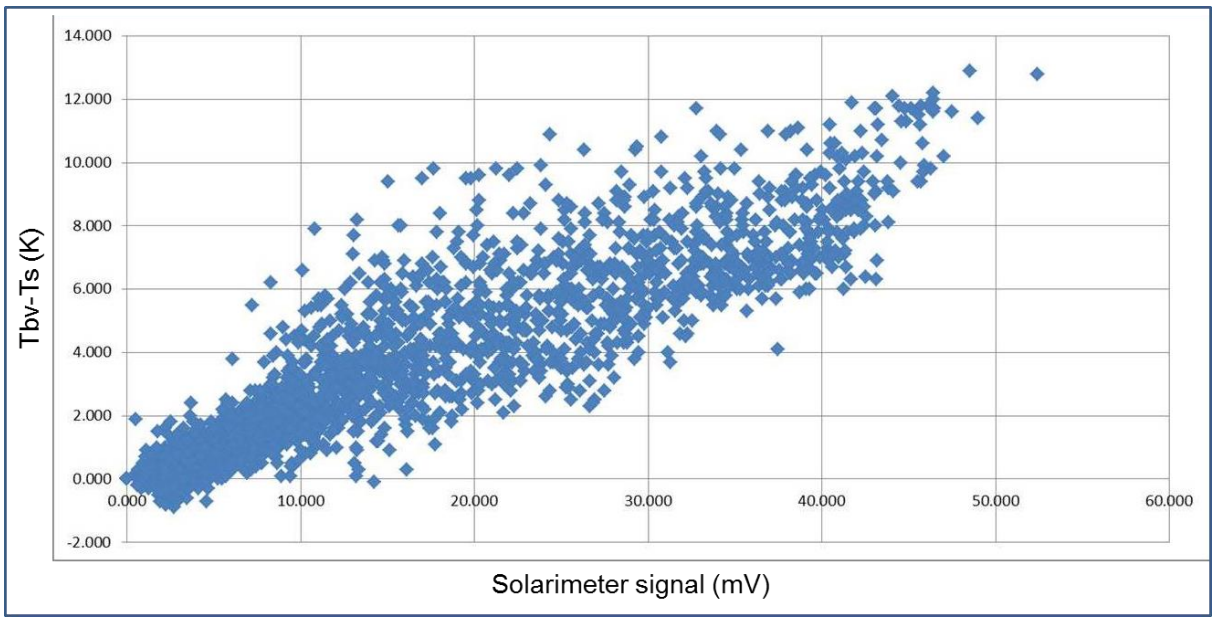

Figure 33 - Relationship between the vial setup and the solarimeter

The following graph (Figure 34) shows how T_{bv}-T_s and the solarimeter signals vary with time. Note that while the solarimeter signal is always zero or positive, the value of T_{bv}-T_s can be negative at night.

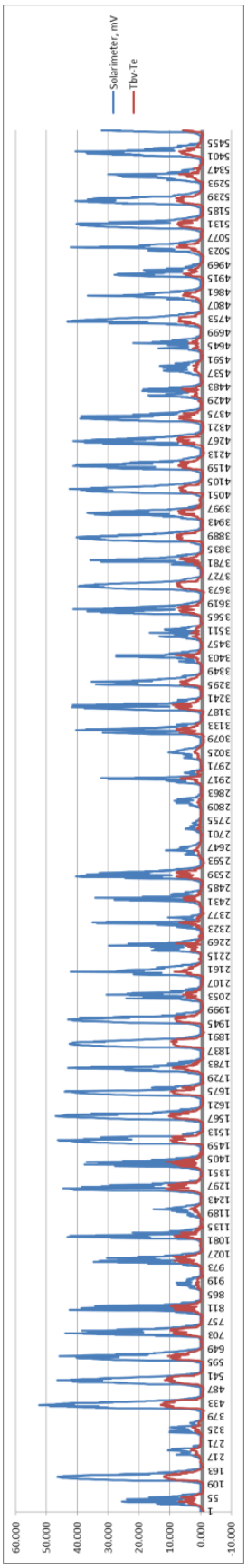

Figure 34 - Time trace of the vial setup and solarimeter

Although the glass vial (which provided a kind of greenhouse effect in order to magnify the temperature difference) gave a satisfactory means of identifying the sunny periods and cloudy periods, it is not clear how practical the use of a glass vial would be in the field. Therefore, a similar test was conducted using a black sensor (i.e. sensor covered using black electrical tape) which was not encased in a glass vial. The correlation was found to be 0.84K instead of 0.91K, suggesting that the glass vial is not strictly necessary for obtaining a good correlation between the temperature difference and the solar radiation as recorded by the solarimeter, though it does improve the ability to identify the times when the sun is shining.

An external surface temperature sensor was glued to the south wall. Brick dust was glued to the surface sensor in order to provide it with a similar albedo and emissivity as the surface of the wall. The cable was taped along the surface of the wall to minimise heat conduction along the cable.

Figure 35 - The external surface sensor

Table 14 summarises results of U-value measurements carried out on the south wall of the test dwelling. The U-values were calculated for each consecutive five-day period, for four locations, indicated as #1, #2, #3 and #4. Position #1 was located farthest to the left (looking from inside) and therefore farthest to the east. Owing to the shape of the property, positions #1 and #2 were likely to be shaded during the mornings, at least for the times of the year when the sun angle was not very high. It is notable that the U-values hovered around 1.6 W/m²K at the colder times of the monitoring period, but tended to be less during the warmer weather. T_{bv}-T_s is the difference in temperature between the black sensor in the vial and the silvery sensor, and is an indicator of the level of sunshine. T_i-T_s is the difference between the indoor temperature and the temperature of the silvery sensor outside. It is noted that the U-values tend to be around 1.6 W/m²K for those cases where T_i-T_s is at least 10 K, but tend to be lower for those cases where T_i-T_s is below 10 K. As would be expected, the U-values tend to be less reliable as we move from springtime into summer, despite the fact that the dwelling is heated continuously.

Table 14 - U-value results on the south facade

Start date	Finish date	U, #1 (W/m²K)	U, #2 (W/m²K)	U, #3 (W/m²K)	U, #4 (W/m²K)	T_{bv}-T_s (K)	T_i-T_s (K)	U mean (W/m²K)
27/02	03/03	1.71	1.64	1.51	1.75	1.78	12.79	1.65
04/03	08/03	1.62	1.57	1.34	1.51	2.85	10.07	1.51
09/03	13/03	1.07	1.11	0.90	1.02	3.29	9.41	1.03
14/03	18/03	0.67	0.78	0.54	0.48	3.76	8.16	0.62
19/03	23/03	1.70	1.68	1.36	1.52	3.32	10.27	1.56
24/03	28/03	1.64	1.59	1.45	1.72	2.17	12.78	1.60
29/03	02/04	0.90	0.87	0.75	0.91	2.48	5.57	0.86
03/04	07/04	1.55	1.52	1.31	1.52	1.12	6.64	1.48
08/04	12/04	0.83	0.87	0.66	0.66	2.58	7.91	0.76
13/04	17/04	0.55	0.61	0.36	0.35	3.46	8.12	0.47
18/04	22/04	1.30	1.33	0.99	1.13	1.69	9.06	1.18
23/04	27/04	1.34	1.35	1.08	1.23	1.47	7.46	1.25
28/04	02/05	1.04	1.07	0.94	1.08	1.22	7.70	1.03
03/05	07/05	0.82	0.88	0.59	0.62	2.52	6.80	0.73
08/05	12/05	1.55	1.53	1.20	1.31	1.29	6.86	1.40
13/05	17/05	0.61	0.58	-0.05	-0.07	1.88	4.85	0.27
18/05	22/05	0.22	0.22	-0.29	-0.30	1.54	3.82	-0.04
23/05	27/05	1.28	1.34	1.21	1.35	0.69	6.91	1.30
28/05	01/06	1.31	1.33	1.04	1.19	0.79	5.05	1.22
02/06	06/06	0.85	0.87	0.42	0.37	1.31	4.83	0.63
07/06	11/06	-0.39	-0.36	-0.90	-0.95	1.58	2.81	-0.65
12/06	16/06	-0.18	-0.03	-0.40	-0.43	1.02	3.61	-0.26
17/06	21/06	-0.37	-0.26	-0.69	-0.71	1.36	2.66	-0.51

The U-values were also derived on the basis of the Stevenson screen temperatures, the silvery thermistor temperatures and the external surface sensor temperatures (note that the external surface sensor was installed later during the monitoring period). The results of this are presented in Appendix C. The table shows U-values calculated from successive five-day periods, using the three different methods of determining the external temperature. Good agreement is observed between the readings from the Stevenson screen and readings from the silvery sensor, but poor agreement is observed regarding the external surface sensor. Closer examination of the data shows that during the afternoons the surface temperature sensor is often above 30 degrees C.

It is notable from Appendix C that even as late as late March the U-values are relatively steady, albeit surprisingly high. In April, all of the U-values appear to fluctuate a great deal, perhaps due to the distortions caused by high sunlight levels and relatively low temperature differences. If anything (as shown below) the U-values obtained from using the external surface sensor are slightly closer to being right than the U-values obtained using the air temperatures.

The following table shows the U-values that were obtained using external surface temperatures for the south wall. It is notable that the U-values, to begin with, are close to 2.2 W/m²K, particularly for the cases where T_{bv}-T_s is low and T_{ai}-T_{br} is high (T_{bv} is the temperature of the black sensor in the glass vial, T_s is the external air temperature measured using a silvery sensor next to the south façade and T_{br} is the external surface temperature measured using the surface sensor that had brick dust covering it).

Table 15 - U-values at position 1, calculated using external surface temperatures (T_{br})

		T_{bv}-T_s	T_{ai}-T_{br}, #1	flux, #1	U, #1
Start	End		K	W/m²	W/m²K
-	03/03	1.78	-	21.84	-
03/03	08/03	2.85	-	16.27	-
08/03	13/03	3.29	4.04	10.06	2.489
13/03	18/03	3.76	2.56	5.43	2.122
18/03	23/03	3.32	6.40	17.44	2.727
23/03	28/03	2.17	9.04	20.96	2.318
28/03	02/04	2.48	1.78	5.04	2.822
02/04	07/04	1.12	4.83	10.29	2.129
07/04	12/04	2.58	2.33	6.54	2.802
12/04	17/04	3.46	1.15	4.46	3.868
17/04	22/04	1.69	4.82	11.75	2.438
22/04	27/04	1.47	4.17	9.96	2.386
27/04	02/05	1.01	7.59	8.00	1.055
02/05	07/05	2.52	1.65	5.58	3.374
07/05	12/05	1.30	4.09	10.62	2.597
12/05	17/05	1.88	-0.73	2.97	-4.047
17/05	22/05	1.54	0.06	0.84	13.530
22/05	27/05	0.69	4.64	8.84	1.906
27/05	01/06	0.79	1.87	6.62	3.532
01/06	06/06	1.31	0.99	4.09	4.148
06/06	11/06	1.58	-1.45	-1.09	0.752
11/06	16/06	1.02	-0.37	-0.65	1.755
16/06	21/06	1.36	-1.71	-0.99	0.580

In conclusion, the temperatures in the glass vial and stainless steel thermistor can give a qualitative indication of sunshine levels. The glass vial, however, might not be very practicable to use in the field unless it is secured very tightly to eliminate the risk of it coming loose during a storm and causing damage to persons, pets or property. It may be worthwhile, in a future set of tests, to try using multiple layers of thin polythene as a substitute for the glass vial, and determining (using the solarimeter readings) whether the greenhouse effect (or polytunnel effect) caused by the multiple layers of cling film could serve as a substitute for a glass vial.

6 Test 6 – Temperature stratification with respect to height

This test looks at the possible effects of height-related stratification in the air temperature. It arises from the question of whether the height above the floor, at which a U-value is measured, could have an impact on the measurements. The current methodology does, however, stipulate that an internal temperature sensor is used beside every heat flux plate in order to minimise the effect of stratification.

This test was conducted in response to some discussion regarding the appropriate positioning of heat flux plates in relation to height above the floor, or distance below the ceiling. For this test, U-values were measured at various heights. The HFPs were placed at different heights on the west wall of the test dwelling as in Figure 36 below.

Figure 36 - Vertical stratification test setup

The results showed that a slightly higher U-value was obtained if the measurement was carried out nearer the ceiling whereas a slightly lower U-value was obtained if the measurement was carried out nearer the floor. This was the case despite the fact that the indoor temperatures adjacent to each heat flux plate were measured.

The results also showed that the difference in the U-value, measured at different heights on the wall, is generally small in the colder months and that the degree of stratification is only large during the warmer months, when U-value measurements are unreliable anyway. Figure 37 below shows the results for the

individual periods of monitoring; confirming that the U-values vary little vertically in the colder months. The three series; “high”, “medium” and “low” refer to the positioning of the groups of HFPs on the wall.

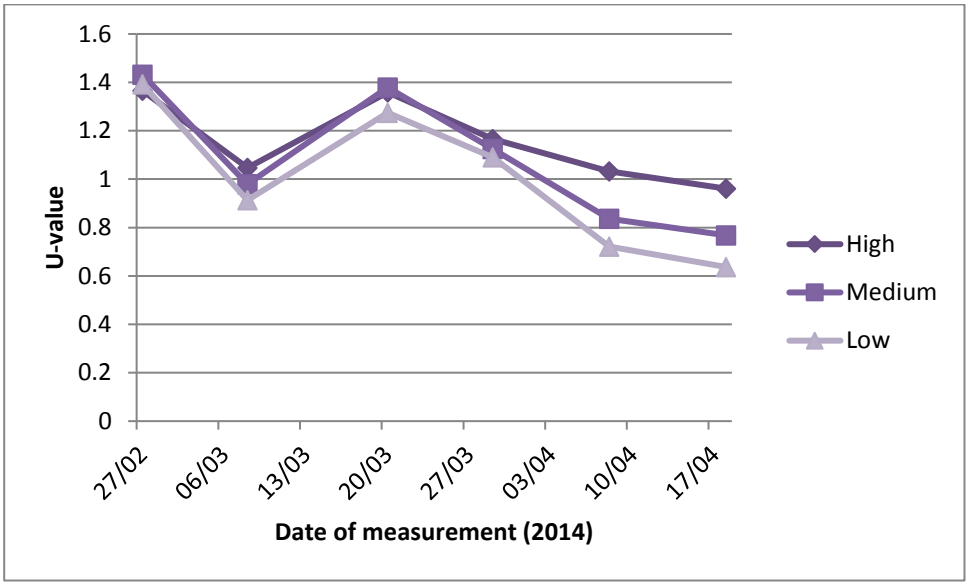

Figure 37 - U-value over time as measured at different heights on the wall

Higher U-values for locations near the ceiling might be explained by thermal bridging. Figure 38 shows the results of thermal modelling of a generalised situation where the ceiling is below a heat-loss roof. The images below show (a) the material properties assumed (b) the predicted temperature distribution and (c) the predicted heat flow. It is notable that the heat flow lines entering the wall are slightly closer together at the top of the wall (leading to higher U-values) than they are lower down.

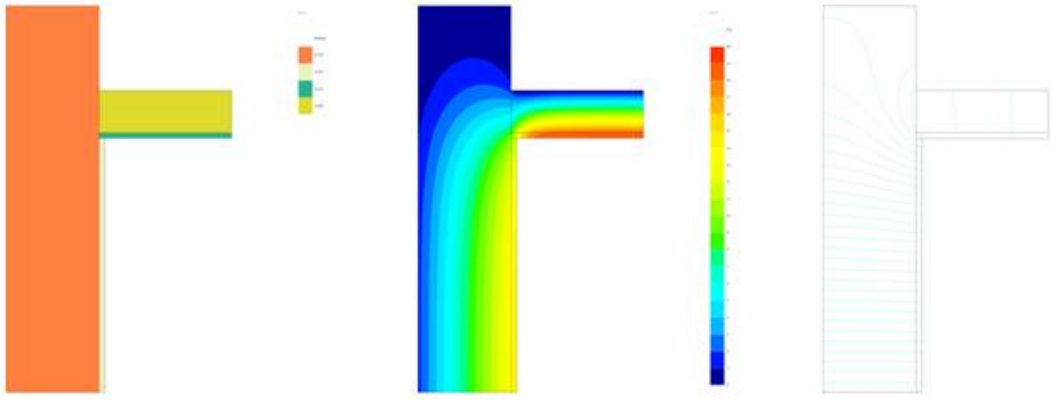

Figure 38 - Thermal model of wall-ceiling junction

The heat flow lines are magnified in the figure below, which indicate that the spacing of the 1-watt-per-metre lines is 22 mm at a distance of 200 mm below the ceiling, but falls to 21 mm at a distance of 100 mm below the ceiling and 18 mm at a distance of 50 mm below the ceiling. In the actual test, the uppermost heat flux plates were at least 300 mm below the ceiling which in this case was below another flat. Therefore the distortion due to thermal bridging, which is likely to be quite small, would not explain the U-values at the top being higher than the U-values at mid storey height.

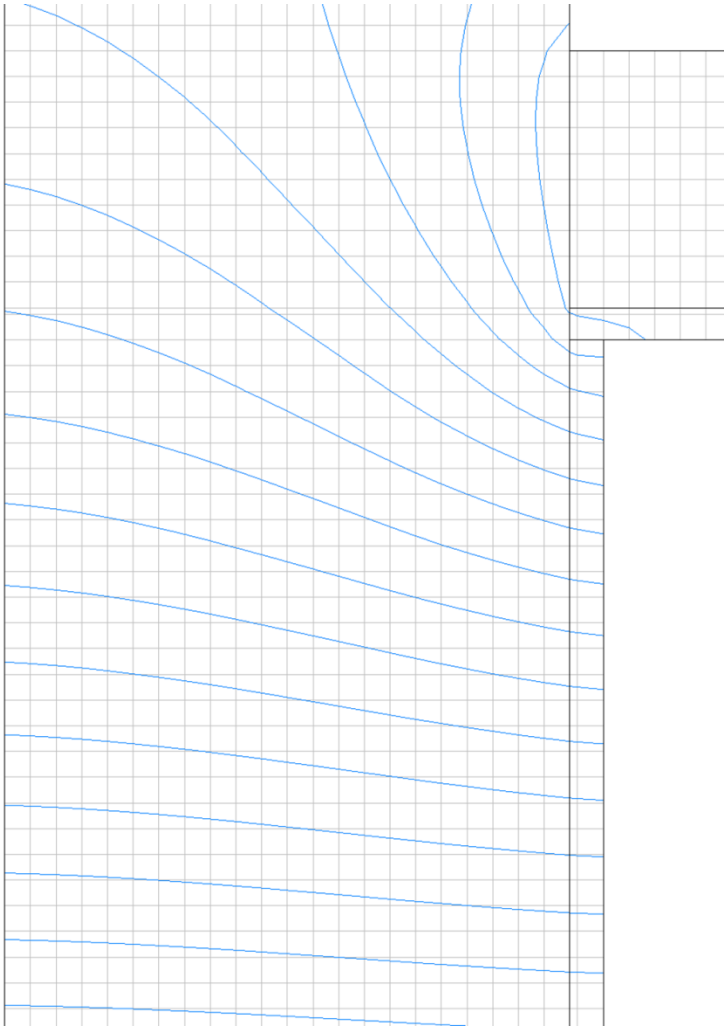

Figure 39 - Heat flow lines predicted by thermal model

In summary, the results of this test suggest that, in the winter months at least, the height at which U-values are measured does not appear to be critical, provided the point of measurement is at least 200mm from the ceiling and at least 200mm from the floor, and provided the indoor temperature is measured at the same height at the heat flux plate. In warmer months there does appear to be a greater difference in U-value when measured at different heights but in any case the U-value measurement is generally unreliable at warmer times of the year.

7 Test 7 – Temperature stratification with respect to distance from wall

This test looks at the possible effects of stratification in the indoor air temperature with respect to the distance from the internal surface of a wall. It examines how critical the distance of the T_{ai} probe (the probe for measuring indoor air temperatures) from the wall surface is. Thermistors were used to monitor temperatures simultaneously, all at the same height above the floor, but at varying distances from the wall. Each of these alternative temperature measurements was then used to calculate a U-value for the wall so that the influence of the distance of the thermistor from the wall could be quantified.

There are not currently strict guidelines about the positioning of the indoor temperature sensors. It is generally assumed that the distance is not critical. This test seeks either to verify that distance is not critical, or to determine what an appropriate minimum distance from the wall is.

Temperatures were measured continuously at mid-storey height, at three locations:

- at 10mm from the surface of the wall
- at around 100mm from the surface of the wall
- at around 500mm from the surface of the wall

Table 16 shows the mean recorded temperatures for each month, for the three distances from the surface of the wall, all at the same height above the floor. It is clear that while the mean temperatures at distances of 480mm and 110mm from the wall surface are similar, the mean temperature at a distance of only 10mm from the wall is lower; at least during the colder months. It appears that as the external temperature increases, this difference decreases and if we had continued the monitoring through the summer we may even have seen the temperature close to the wall surface exceed that of the indoor air.

Table 16 - Average temperatures at different distances from wall surface

Distance from wall surface	**mm**	**480**	**110**	**10**	**ext. air**
March temperatures	DegC	22.13	22.14	21.93	10.98
April temperatures	DegC	22.17	22.18	22.00	12.99
May temperatures	DegC	22.20	22.21	22.09	14.66
June temperatures	DegC	23.45	23.41	23.44	18.62

Table 17 shows the differences between the internal temperature and the external temperature at the same three distances from the internal surface of the wall.

Table 17 - Internal - external temperature differences

Distance from wall surface	mm	480	110	10
T_i - T_e, March	DegC	11.15	11.16	10.95
T_i - T_e, April	DegC	9.18	9.19	9.02
T_i - T_e, May	DegC	7.54	7.55	7.43
T_i - T_e, June	DegC	4.83	4.78	4.82

It is evident from the above table, that if the indoor temperature is monitored at a distance of only 10mm from the wall's surface, instead of farther in towards the centre of the room, the difference in temperature between inside and outside could be underestimated by up to 2%. This could lead us to overestimating the U-value by up to 2%.

Figure 40shows the results of an additional test which was carried out in early 2015, in a different property, showing the trend between air temperature and distance from a wall, showing that although a significant drop in temperture is seen close to the surface of an external wall, the distortion to the temperature is much less if the distance of the temperature sensor from the wall is at least 20 mm.

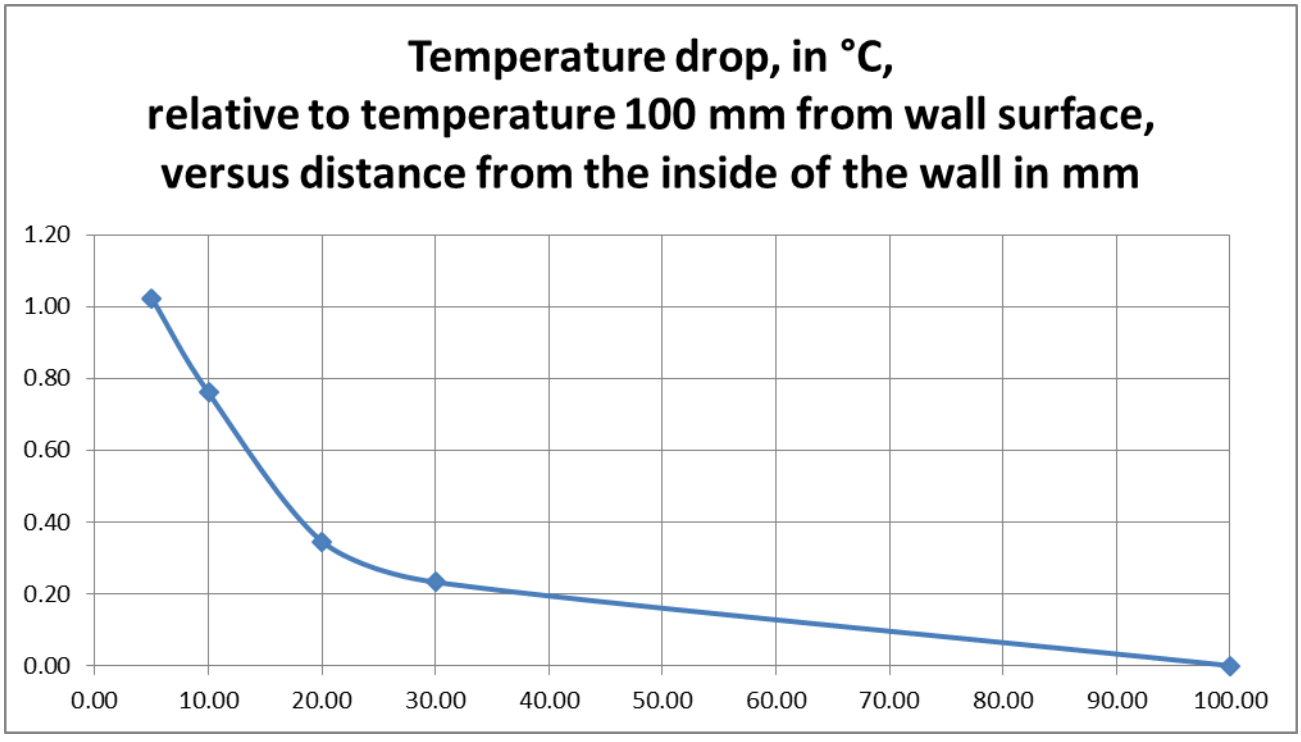

Figure 40 - The drop in air temperature in relation to distance from a wall

In conclusion, the above suggests that the thermistor and its wire should always be at least 10mm from the wall's internal surface, and preferably a little more, say at least 20mm.

8 Summary assessment of the HFP methodology

The methodology for assessing in situ U-value measurements consisted of seven tests in both laboratory and field settings. These are:

1. The comparison of the in situ method with hot-box measurements
2. The impact of surface texture on accuracy
3. Reproducibility of the substrate to the heat flow sensor
4. The method of affixing the sensor to a wall
5. The impact of direct sunlight on a measured U-value
6. Stratification of indoor temperature with respect to height
7. Stratification of indoor temperature with respect to distance from a wall

Tests 1 & 2 were carried out in NPL's (National Physical Laboratory) rotatable hot-box, tests 3 to 7 were carried out in a vacant dwelling with a controlled indoor environment.

Test 1 concluded that the U-values obtained using the in situ HFP methodology compared well with those obtained using the hot-box methodology but that there is a small systematic bias towards underestimating the wall U-value. There therefore needs to be a positive correction applied to HFP U-value measurements. This paper argues that an appropriate correction would be +5.0%.

Test 2, carried out at the same time as test 1, showed that the application of Vaseline and Clingfilm provided good thermal contact between the HFP and the surface of a wall, whether the surface is smooth or uneven (for example decorated with embossed wallpaper). This enabled a correct heat flux to be measured and hence a correct U-value measurement to be produced.

Test 3 sought to establish whether the way that Vaseline is applied to the heat flux plate might cause inconsistencies to the measurement of U-values. The results showed that this is not the case. It is possible to achieve consistent U-value measurements when removing and reapplying the substrate; even when the work is being undertaken by different people.

Test 4 compared the pressure-fixing method (used for all measurements undertaken for this project) to the use of adhesive tape (both double-sided tape and duct tape). It showed that it is difficult to obtain sensible readings of any kind using double-sided tape in an environment with dusty or unclean surfaces, such as was the case for our test house in West London. The use of duct tape stuck over the front of the HFP did provide a better contact with the wall however the presence of the tape itself had an effect on the measured U-value. Possible reasons for this are the creation of air pockets around the HFP or the reduced emissivity compared to having no tape on the plate.

Test 5 investigated how well the method works when trying to measure U-values in warmer and sunnier months. Guidance states that U-values are best taken when external temperatures are low and the difference between inside and outside is high, however it is of interest to see what is possible when this is not the case. The results showed that U-values tended to be fairly stable when the temperature difference between inside and outside was over 10K. There is also some indication that it might be possible to obtain sensible U-value measurements when the temperature difference is less than 10K (in other words in warmer months) provided that the sun isn't shining on the wall. The results for this are still only indicative and more work would be needed before we could justify measuring U-values in milder

external conditions. What can be concluded is that if it is necessary to measure U-values on an unshaded south façade, it is advisable to measure for longer than the recommended two weeks in order to achieve enough measurements on days when conditions are suitable i.e. periods with little or no solar radiation. This test also showed that it is possible to detect when the sun is shining with relatively low-cost equipment such as black thermistors in glass vials.

Test 6 questioned whether it is important to measure U-values at a particular height on the inside wall surface. The results indicated that vertical position does not materially affect the measured U-value, as long as the HFP is placed at least 200mm from the ceiling and the floor and provided that the internal temperature is measured adjacent to the HFP.

Test 7 asked whether there is an ideal distance from the wall at which to measure the internal air temperature. It looked at the U-values resulting from temperatures measured at 10mm, 100mm and 500mm from the wall surface. The results suggested that in colder months, the temperature could be as much as 2% lower at a distance of 10mm which would lead to a 2% overestimation of U-value. It is therefore recommended that temperatures are measured at least 20mm from the wall surface.

Taken together, these tests can be considered to have validated the technology used to measure in situ U-values; namely the HFP01 heat flux plates and associated equipment, as well as the methodology used to undertake measurements. More is now known about the constraints of the method; such as its use in summer months, and of its components; such as the positioning of temperature sensors.

9 References

1. BS EN ISO 6946:2007 “Building components and building elements - Thermal resistance and thermal transmittance - Calculation method”
2. Rhee-Duverne S and Baker P, , “Research into the thermal performance of traditional brick walls, English Heritage Research report” 2013

Appendix A Calculated thermal resistance and U-value of test panel

U-value calculation
by BRE U-value Calculator version 2.03e

NPL Test panel

Layer	d (mm)	λ layer	λ bridge	Fraction	R layer	R bridge	Description
					0.130		Rsi
1	12.5	0.160			0.078		Plasterboard
2	13	0.034			0.382		EPS Insulation
3	12.5	0.160			0.078		Plasterboard
					0.040		Rse
	38 mm (total wall thickness)				0.709		

Total resistance: Upper limit: 0.709 Lower limit: 0.709 Ratio: 1.000 Average: 0.709 m²K/W

U-value 1.411

U-value (rounded) 1.41 W/m²K

Test panel thermal conductance

This is the conductance of the test panel (i.e. resistance of the panel without the internal and external surface resistances).

Layer	d (mm)	λ layer	λ bridge	Fraction	R layer	R bridge	Description
1	12.5	0.160			0.078		Plasterboard
2	13	0.034			0.382		EPS Insulation
3	12.5	0.160			0.078		Plasterboard
	38 mm (total wall thickness)				0.538		

Thermal conductance is 1/0.538 = 1.859 W/m²K

Appendix B Calculation of heat flux through the HFP01 sensor

The following images and corresponding tables show the calculated heat fluxes through the HFP01 sensor for the various set-ups.

Calibration set-up

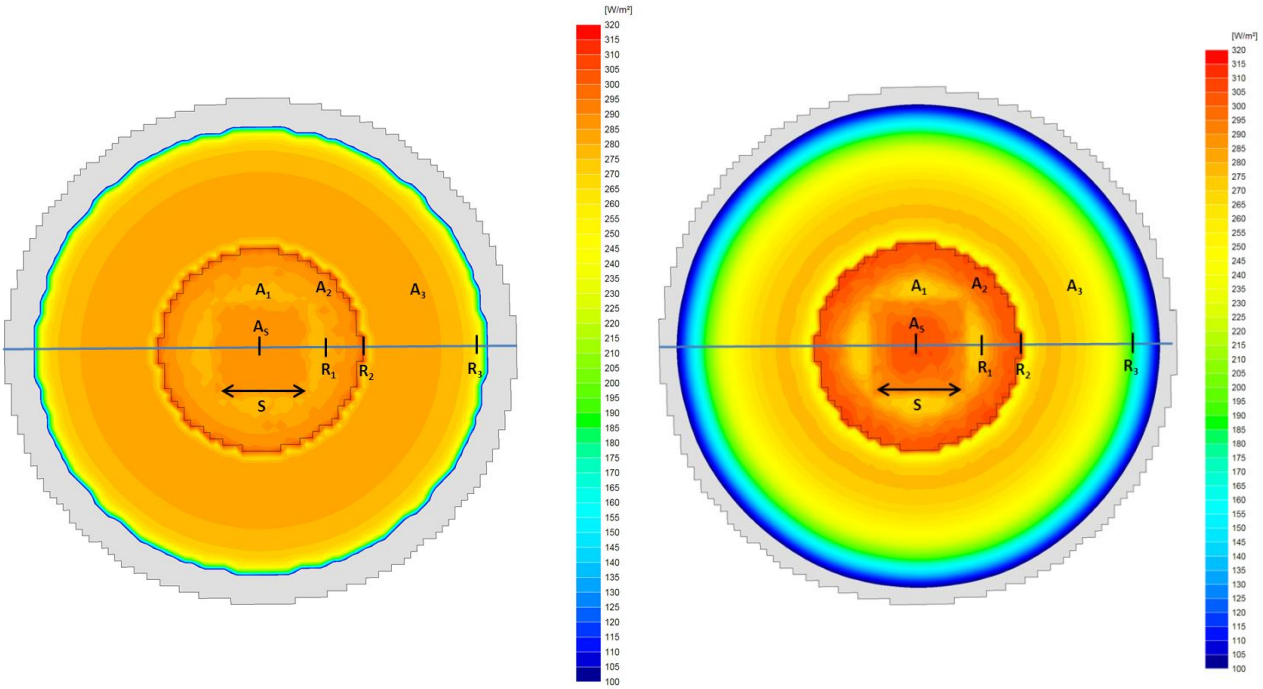

Hot-side							
	Dimension		Area		Flux		Power
	(mm)		(m²)		(W/m²)		(W)
S	14.8	A_S	0.000219	Φ_S	285	P_S	0.0624
R_1	11	A_1	0.000161	Φ_1	265	P_1	0.0427
R_2	16	A_2	0.000424	Φ_2	285	P_2	0.1209
R_3	35	A_3	0.003044	Φ_3	275	P_3	0.8372
		Total:	0.003848	Φ_{HFP}	276	P_{Total}	1.0631
				Φ_S/Φ_{HFP} :	1.032		
Cold-side							
	Dimension		Area		Flux		Power
	(mm)		(m²)		(W/m²)		(W)
S	14.8	A_S	0.000219	Φ_S	290	P_S	0.0635
R_1	11	A_1	0.000161	Φ_1	265	P_1	0.0427
R_2	16	A_2	0.000424	Φ_2	285	P_2	0.1209
R_3	35	A_3	0.003044	Φ_3	265	P_3	0.8067
		Total:	0.003848	Φ_{HFP}	269	P_{Total}	1.0338
				Φ_S/Φ_{HFP} :	1.080		
				Ave Φ_S/Φ_{HFP} :	**1.056**		

Hot-box* test panel *set-up

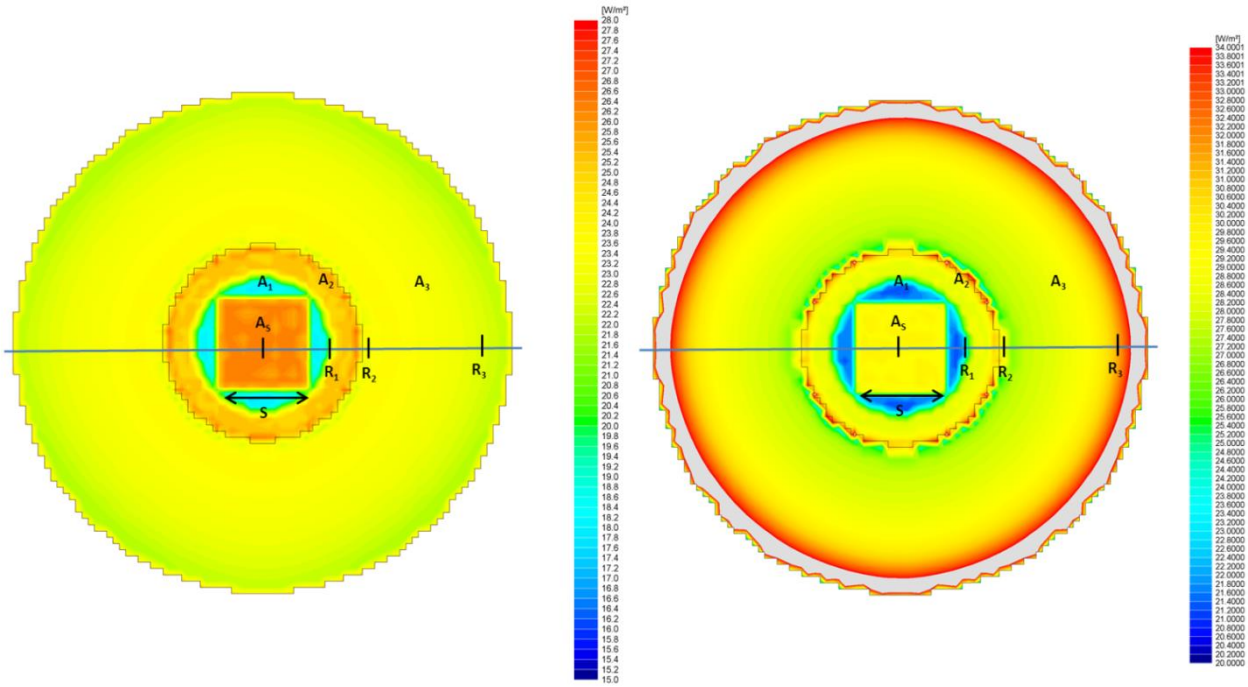

Hot-side							
	Dimension		Area		Flux		Power
	(mm)		(m^2)		(W/m^2)		(W)
S	14.8	A_S	0.000219	Φ_S	25.8	P_S	0.005651
R_1	11	A_1	0.000161	Φ_1	18.6	P_1	0.002996
R_2	16	A_2	0.000424	Φ_2	24.8	P_2	0.010518
R_3	35	A_3	0.003044	Φ_3	23.6	P_3	0.071843
		Total:	0.003848	Φ_{HFP}	23.6		0.091009
				Φ_S/Φ_{HFP} :	1.091		
Cold-side							
	Dimension		Area		Flux		Power
	(mm)		(m^2)		(W/m^2)		(W)
S	14.8	A_S	0.000219	Φ_S	28.8	P_S	0.006308
R_1	11	A_1	0.000161	Φ_1	21.8	P_1	0.003512
R_2	16	A_2	0.000424	Φ_2	29.2	P_2	0.012384
R_3	35	A_3	0.003044	Φ_3	29.0	P_3	0.088282
		Total:	0.003848	Φ_{HFP}	28.7		0.110486
				Φ_S/Φ_{HFP} :	1.003		
Averages from Hot-side and cold side heat fluxes							**%**
				Φ_S/Φ_{HFP} :	1.047	$S_{1\ error}$	-7.2
				Φ_{HFP}:	26.179	$S_{2\ error}$	-0.8
				$\Phi_{undisturbed}$:	28.22	S_{Total}	-8.0

In situ Solid wall set-up

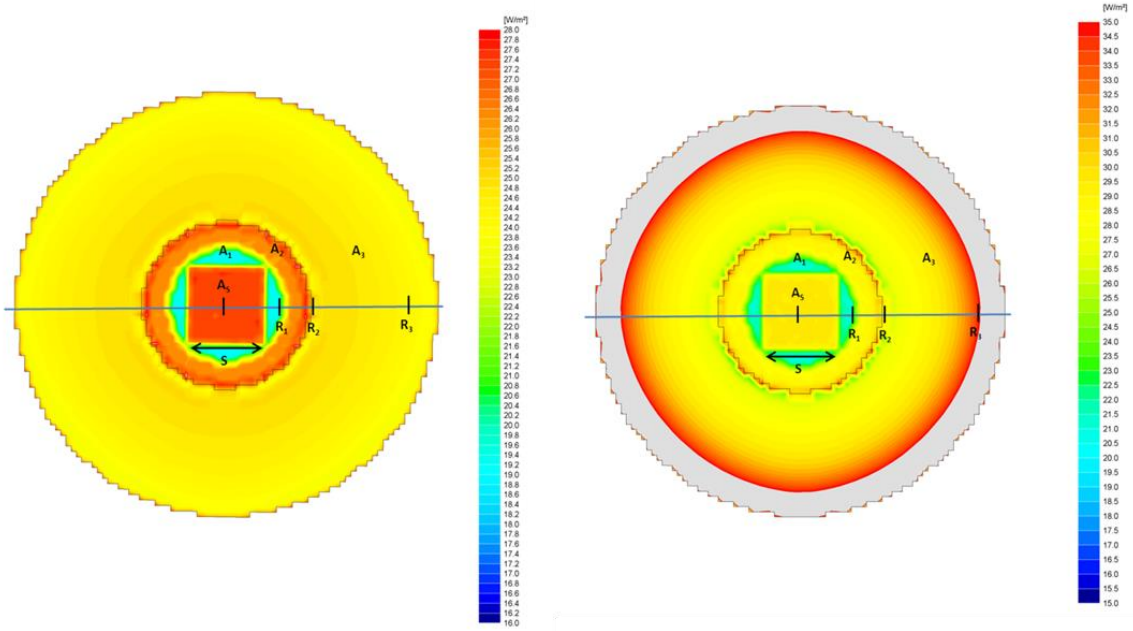

Hot-side							
	Dimension		Area		Flux		Power
	(mm)		(m²)		(W/m²)		(W)
S	14.8	A_S	0.000219	Φ_S	28.5	P_S	0.006133
R_1	11	A_1	0.000161	Φ_1	21.0	P_1	0.003383
R_2	16	A_2	0.000424	Φ_2	28.5	P_2	0.011875
R_3	35	A_3	0.003044	Φ_3	29.5	P_3	0.088282
		Total:	0.003848	Φ_{HFP}	29.0		0.109673
				Φ_S/Φ_{HFP} :	0.984		
Cold-side							
	Dimension		Area		Flux		Power
	(mm)		(m²)		(W/m²)		(W)
S	14.8	A_S	0.000219	Φ_S	26.8	P_S	0.005870
R_1	11	A_1	0.000161	Φ_1	20.0	P_1	0.003222
R_2	16	A_2	0.000424	Φ_2	26.2	P_2	0.011112
R_3	35	A_3	0.003044	Φ_3	24.2	P_3	0.073670
		Total:	0.003848	Φ_{HFP}	24.4		
				Φ_S/Φ_{HFP} :	1.099		
Averages from Hot-side and cold side heat fluxes							**%**
				Φ_S/Φ_{HFP} :	1.041	$S_{1\ error}$	-6.0
				Φ_{HFP}:	26.685	$S_{2\ error}$	-1.4
				$\Phi_{undisturbed}$:	28.38	S_{Total}	-7.4

Appendix C U-values calculated with alternative external temperature values

Start	End	U-value using temperature of Stevenson screen					U-value using temperature of Silver thermistor					U-value using of external surface temperature				
		#1	#2	#3	#4	Ti-Te	#1	#2	#3	#4	Ti-Te	#1	#2	#3	#4	Ti-Te
26/02	03/03	1.70	1.64	1.50	1.74	12.55	1.71	1.64	1.51	1.75	12.50	-	-	-	-	-
27/02	04/03	1.70	1.65	1.53	1.79	12.93	1.72	1.66	1.55	1.81	12.81	-	-	-	-	-
28/02	05/03	1.71	1.65	1.47	1.69	12.55	1.75	1.68	1.50	1.73	12.32	-	-	-	-	-
01/03	06/03	1.74	1.67	1.39	1.58	11.89	1.78	1.71	1.42	1.61	11.64	-	-	-	-	-
02/03	07/03	1.73	1.66	1.39	1.57	11.21	1.78	1.71	1.43	1.62	10.91	-	-	-	-	-
03/03	08/03	1.56	1.51	1.30	1.45	10.23	1.62	1.57	1.34	1.51	9.86	-	-	-	-	-
04/03	09/03	1.37	1.36	1.13	1.24	9.05	1.43	1.42	1.18	1.30	8.63	-	-	-	-	-
05/03	10/03	1.12	1.15	0.98	1.07	8.92	1.18	1.21	1.03	1.12	8.50	-	-	-	-	-
06/03	11/03	1.16	1.21	1.10	1.25	9.09	1.20	1.26	1.15	1.30	8.72	-	-	-	-	-
07/03	12/03	1.15	1.19	1.03	1.17	9.36	1.20	1.24	1.08	1.23	8.96	-	-	-	-	-
08/03	13/03	1.02	1.07	0.87	0.98	9.67	1.07	1.11	0.90	1.02	9.27	-	-	-	-	-

09/03	14/03	0.96	1.00	0.80	0.90	10.11	1.00	1.04	0.84	0.93	9.73	-	-	-	-	-
10/03	15/03	0.91	0.97	0.80	0.88	9.53	0.95	1.01	0.83	0.92	9.14	-	-	-	-	-
11/03	16/03	0.62	0.71	0.48	0.46	8.64	0.66	0.75	0.50	0.49	8.15	-	-	-	-	-
12/03	17/03	0.40	0.52	0.32	0.26	8.59	0.42	0.55	0.33	0.27	8.14	-	-	-	-	-
13/03	18/03	0.63	0.74	0.51	0.46	8.52	0.67	0.78	0.54	0.48	8.11	-	-	-	-	-
14/03	19/03	0.91	1.00	0.79	0.79	8.40	0.95	1.04	0.83	0.83	8.05	-	-	-	-	-
15/03	20/03	1.17	1.23	1.02	1.08	8.55	1.21	1.27	1.06	1.12	8.27	-	-	-	-	-
16/03	21/03	1.42	1.44	1.19	1.30	9.17	1.45	1.47	1.22	1.34	8.95	-	-	-	-	-
17/03	22/03	1.66	1.65	1.33	1.48	9.59	1.70	1.69	1.36	1.51	9.36	-	-	-	-	-
18/03	23/03	1.65	1.64	1.32	1.47	10.32	1.70	1.68	1.36	1.52	10.04	-	-	-	-	-
19/03	24/03	1.57	1.56	1.21	1.34	11.15	1.61	1.60	1.25	1.39	10.84	-	-	-	-	-
20/03	25/03	1.56	1.55	1.22	1.36	11.81	1.59	1.58	1.25	1.39	11.55	2.62	2.62	2.07	2.41	6.90
21/03	26/03	1.57	1.55	1.32	1.51	12.74	1.59	1.58	1.34	1.54	12.52	2.42	2.41	2.05	2.44	8.14
22/03	27/03	1.57	1.54	1.36	1.60	12.93	1.60	1.57	1.39	1.63	12.73	2.37	2.34	2.07	2.53	8.45
23/03	28/03	1.62	1.57	1.43	1.70	12.54	1.64	1.59	1.45	1.72	12.39	2.32	2.26	2.06	2.54	8.66
24/03	29/03	1.68	1.61	1.49	1.80	11.22	1.70	1.63	1.51	1.83	11.06	2.45	2.36	2.20	2.76	7.56

25/03	30/03	1.58	1.50	1.37	1.67	9.89	1.62	1.53	1.41	1.71	9.65	2.63	2.51	2.32	2.98	5.81
26/03	31/03	1.48	1.40	1.25	1.52	8.08	1.52	1.44	1.29	1.57	7.84	2.64	2.51	2.26	2.92	4.44
27/03	01/04	1.23	1.18	1.07	1.29	6.75	1.28	1.22	1.11	1.34	6.52	2.74	2.63	2.42	3.20	2.95
28/03	02/04	0.87	0.83	0.72	0.87	5.72	0.90	0.87	0.75	0.91	5.48	2.82	2.70	2.36	3.26	1.70
29/03	03/04	0.74	0.72	0.64	0.76	5.64	0.76	0.75	0.66	0.79	5.47	1.85	1.80	1.61	2.06	2.22
30/03	04/04	0.88	0.87	0.78	0.91	5.90	0.90	0.89	0.80	0.93	5.76	1.83	1.80	1.64	2.02	2.79
31/03	05/04	1.03	1.00	0.89	1.01	6.34	1.05	1.03	0.91	1.04	6.16	2.16	2.11	1.87	2.29	2.96
01/04	06/04	1.29	1.26	1.06	1.23	6.31	1.31	1.28	1.08	1.25	6.20	2.05	2.00	1.70	2.04	3.92
02/04	07/04	1.54	1.51	1.30	1.51	6.52	1.55	1.52	1.31	1.52	6.48	2.13	2.09	1.81	2.16	4.67
03/04	08/04	1.64	1.60	1.35	1.54	7.22	1.66	1.62	1.37	1.56	7.13	2.41	2.36	1.99	2.36	4.86
04/04	09/04	1.59	1.56	1.25	1.39	7.47	1.63	1.59	1.28	1.42	7.33	2.88	2.83	2.27	2.67	4.07
05/04	10/04	1.34	1.32	1.00	1.06	7.43	1.37	1.35	1.02	1.09	7.26	3.25	3.21	2.41	2.77	3.01
06/04	11/04	0.99	1.01	0.76	0.78	7.73	1.02	1.04	0.79	0.81	7.49	3.13	3.22	2.40	2.69	2.39
07/04	12/04	0.79	0.84	0.64	0.63	8.16	0.83	0.87	0.66	0.66	7.84	2.80	2.98	2.24	2.42	2.27
08/04	13/04	0.63	0.69	0.48	0.45	7.77	0.66	0.72	0.50	0.47	7.43	3.71	4.07	2.78	2.92	1.29
09/04	14/04	0.46	0.54	0.36	0.32	7.93	0.49	0.57	0.37	0.34	7.56	2.82	3.34	2.14	2.11	1.28

10/04	15/04	0.44	0.53	0.38	0.37	8.47	0.46	0.55	0.39	0.39	8.09	2.08	2.51	1.77	1.87	1.76
11/04	16/04	0.51	0.58	0.40	0.40	8.71	0.53	0.61	0.42	0.42	8.31	2.52	2.91	2.01	2.16	1.72
12/04	17/04	0.52	0.58	0.34	0.25	8.52	0.55	0.61	0.36	0.26	8.10	3.87	4.32	2.44	1.98	1.14
13/04	18/04	0.58	0.64	0.36	0.33	9.12	0.61	0.67	0.38	0.35	8.73	2.56	2.83	1.57	1.52	2.06
14/04	19/04	0.77	0.82	0.52	0.64	9.41	0.80	0.85	0.54	0.67	9.08	2.52	2.70	1.68	2.23	2.83
15/04	20/04	0.99	1.04	0.76	1.12	9.35	1.02	1.07	0.78	1.15	9.12	2.19	2.31	1.68	2.62	4.17
16/04	21/04	1.25	1.27	0.92	1.17	8.96	1.27	1.30	0.94	1.20	8.80	2.72	2.79	2.00	2.73	4.05
17/04	22/04	1.28	1.31	0.98	1.11	8.99	1.30	1.33	0.99	1.13	8.89	2.44	2.51	1.86	2.25	4.65
18/04	23/04	1.38	1.40	1.09	1.26	8.35	1.39	1.41	1.10	1.27	8.27	2.50	2.56	1.99	2.43	4.51
19/04	24/04	1.40	1.39	1.04	1.20	7.47	1.40	1.39	1.04	1.20	7.47	2.80	2.79	2.08	2.57	3.67
20/04	25/04	1.32	1.30	0.94	1.07	7.41	1.33	1.30	0.94	1.07	7.39	2.70	2.67	1.92	2.32	3.58
21/04	26/04	1.26	1.26	0.97	1.10	7.48	1.27	1.27	0.97	1.10	7.44	2.26	2.28	1.74	2.07	4.12
22/04	27/04	1.32	1.34	1.07	1.22	7.38	1.34	1.35	1.08	1.23	7.31	2.39	2.42	1.94	2.32	4.03
23/04	28/04	1.25	1.27	1.08	1.25	7.38	1.26	1.28	1.09	1.25	7.33	2.12	2.17	1.85	2.24	4.27
24/04	29/04	1.20	1.25	1.17	1.37	7.49	1.21	1.26	1.19	1.39	7.41	1.81	1.89	1.78	2.16	4.91
25/04	30/04	1.18	1.21	1.08	1.25	6.83	1.21	1.24	1.11	1.29	6.67	2.42	2.48	2.24	2.81	3.26

26/04	01/05	1.02	1.05	0.93	1.06	7.08	1.03	1.06	0.93	1.07	7.04	1.90	1.96	1.74	2.11	3.74
27/04	02/05	1.03	1.06	0.93	1.07	7.59	1.04	1.07	0.94	1.08	7.54	1.81	1.86	1.64	1.98	4.27
28/04	03/05	1.07	1.10	0.92	1.04	8.14	1.08	1.11	0.93	1.05	8.04	2.20	2.27	1.91	2.29	3.88
29/04	04/05	0.98	1.02	0.83	0.91	8.47	1.00	1.04	0.84	0.93	8.34	2.30	2.41	1.95	2.31	3.54
30/04	05/05	0.97	1.04	0.85	0.94	8.46	0.99	1.05	0.87	0.96	8.32	2.08	2.22	1.83	2.15	3.88
01/05	06/05	0.93	0.99	0.76	0.83	7.76	0.97	1.02	0.78	0.86	7.50	2.73	2.90	2.21	2.67	2.60
02/05	07/05	0.79	0.84	0.57	0.60	7.02	0.82	0.88	0.59	0.62	6.75	3.37	3.63	2.40	2.83	1.61
03/05	08/05	0.80	0.86	0.59	0.61	6.37	0.82	0.89	0.61	0.63	6.22	2.21	2.42	1.63	1.80	2.26
04/05	09/05	1.03	1.08	0.75	0.79	5.85	1.06	1.11	0.77	0.81	5.69	2.52	2.66	1.82	2.05	2.36
05/05	10/05	1.13	1.15	0.83	0.87	5.98	1.15	1.17	0.84	0.88	5.91	2.32	2.37	1.68	1.87	2.89
06/05	11/05	1.40	1.41	1.12	1.21	6.59	1.41	1.42	1.13	1.22	6.54	2.19	2.22	1.76	1.96	4.16
07/05	12/05	1.54	1.53	1.20	1.31	6.77	1.55	1.53	1.20	1.31	6.74	2.60	2.58	2.02	2.32	3.97
08/05	13/05	1.38	1.36	1.06	1.15	7.12	1.38	1.36	1.06	1.15	7.10	2.71	2.68	2.08	2.40	3.56
09/05	14/05	1.26	1.24	0.93	0.99	7.31	1.26	1.25	0.93	1.00	7.27	2.93	2.91	2.16	2.48	3.08
10/05	15/05	1.14	1.13	0.74	0.78	6.85	1.16	1.15	0.76	0.80	6.74	4.29	4.28	2.75	3.28	1.78
11/05	16/05	0.84	0.81	0.30	0.30	5.97	0.86	0.83	0.31	0.31	5.84	####	####	17.18	####	0.03

12/05	17/05	0.59	0.56	-0.05	-0.07	5.09	0.61	0.58	-0.05	-0.07	4.92	-4.05	-3.90	0.40	0.62	-0.66
13/05	18/05	0.41	0.31	-0.57	-0.60	3.95	0.44	0.33	-0.62	-0.65	3.66	-0.73	-0.57	1.20	1.40	-1.97
14/05	19/05	0.09	-0.07	-1.13	-1.12	3.17	0.10	-0.08	-1.24	-1.23	2.88	-0.10	0.08	1.55	1.79	-2.39
15/05	20/05	-0.06	-0.17	-1.01	-0.99	3.34	-0.07	-0.19	-1.10	-1.07	3.06	0.12	0.35	2.44	2.91	-1.45
16/05	21/05	0.07	0.02	-0.63	-0.64	3.63	0.08	0.02	-0.68	-0.69	3.36	-0.28	-0.08	3.06	3.95	-0.80
17/05	22/05	0.21	0.21	-0.27	-0.29	4.15	0.22	0.22	-0.29	-0.30	3.92	13.53	11.02	-5.45	-4.38	0.16
18/05	23/05	0.54	0.57	0.23	0.23	4.72	0.56	0.59	0.24	0.23	4.54	1.72	1.84	0.72	0.71	1.49
19/05	24/05	0.78	0.83	0.60	0.62	5.53	0.78	0.84	0.61	0.63	5.47	1.49	1.60	1.15	1.22	2.87
20/05	25/05	1.09	1.14	0.89	0.93	5.57	1.10	1.16	0.90	0.94	5.49	2.11	2.23	1.72	1.87	2.84
21/05	26/05	1.15	1.21	1.03	1.11	6.16	1.14	1.21	1.03	1.11	6.19	1.83	1.94	1.65	1.85	3.82
22/05	27/05	1.29	1.35	1.22	1.36	6.68	1.28	1.34	1.21	1.35	6.74	1.91	2.01	1.82	2.10	4.47
23/05	28/05	1.35	1.42	1.31	1.50	6.97	1.33	1.40	1.30	1.47	7.07	1.95	2.05	1.91	2.26	4.77
24/05	29/05	1.38	1.44	1.33	1.53	6.57	1.37	1.42	1.32	1.52	6.63	2.10	2.19	2.03	2.46	4.26
25/05	30/05	1.30	1.35	1.29	1.49	6.67	1.28	1.33	1.27	1.47	6.77	1.86	1.94	1.86	2.24	4.60
26/05	31/05	1.39	1.42	1.30	1.50	6.09	1.40	1.44	1.31	1.52	6.04	2.34	2.41	2.21	2.73	3.54
27/05	01/06	1.28	1.29	1.01	1.15	5.08	1.31	1.33	1.04	1.19	4.95	3.53	3.60	2.81	3.67	1.78

28/05	02/06	0.93	0.92	0.47	0.51	4.37	0.97	0.96	0.48	0.53	4.21	9.27	9.12	4.07	6.37	0.43
29/05	03/06	0.68	0.71	0.24	0.24	4.47	0.70	0.73	0.25	0.24	4.32	6.90	7.21	2.11	2.35	0.46
30/05	04/06	0.63	0.68	0.24	0.20	4.78	0.64	0.68	0.24	0.20	4.73	4.24	4.48	1.40	1.27	0.75
31/05	05/06	0.76	0.81	0.29	0.24	4.78	0.76	0.81	0.29	0.24	4.78	4.55	4.79	1.53	1.34	0.84
01/06	06/06	0.84	0.87	0.41	0.37	4.91	0.85	0.87	0.42	0.37	4.87	4.15	4.29	1.87	1.79	1.02
02/06	07/06	0.78	0.84	0.52	0.50	4.77	0.78	0.84	0.52	0.50	4.74	2.79	3.00	1.79	1.83	1.33
03/06	08/06	0.79	0.83	0.41	0.37	4.10	0.82	0.85	0.42	0.38	3.99	18.75	18.79	6.53	8.86	0.20
04/06	09/06	0.50	0.51	-0.05	-0.10	3.12	0.53	0.54	-0.05	-0.10	2.95	-1.32	-1.36	0.14	0.29	-1.11
05/06	10/06	-0.18	-0.18	-0.67	-0.71	3.03	-0.19	-0.19	-0.72	-0.75	2.84	0.37	0.38	1.56	1.83	-1.34
06/06	11/06	-0.37	-0.34	-0.86	-0.91	3.08	-0.39	-0.36	-0.90	-0.95	2.92	0.75	0.71	2.01	2.53	-1.34
07/06	12/06	-0.35	-0.37	-1.11	-1.16	2.87	-0.38	-0.40	-1.19	-1.25	2.67	0.43	0.46	1.55	1.93	-2.09
08/06	13/06	-0.47	-0.47	-1.24	-1.25	2.92	-0.51	-0.50	-1.33	-1.34	2.72	0.57	0.58	1.73	2.11	-2.13
09/06	14/06	-0.37	-0.32	-1.00	-1.02	3.43	-0.40	-0.34	-1.06	-1.08	3.23	0.68	0.60	2.12	2.64	-1.66
10/06	15/06	-0.31	-0.18	-0.69	-0.73	3.62	-0.33	-0.19	-0.73	-0.76	3.43	0.92	0.55	2.42	3.16	-1.07
11/06	16/06	-0.17	-0.03	-0.39	-0.41	3.85	-0.18	-0.03	-0.40	-0.43	3.68	1.75	0.27	5.59	9.79	-0.30
12/06	17/06	-0.02	0.10	-0.21	-0.22	4.15	-0.02	0.11	-0.22	-0.23	3.97	0.69	-2.96	21.52	-60.03	-0.08

13/06	18/06	-0.05	0.10	-0.06	-0.07	4.37	-0.05	0.10	-0.06	-0.07	4.22	-0.45	0.88	-0.49	-0.51	0.52
14/06	19/06	0.01	0.16	-0.02	-0.03	4.14	0.02	0.17	-0.02	-0.03	3.92	0.22	2.41	-0.23	-0.38	0.31
15/06	20/06	-0.03	0.11	-0.10	-0.12	3.65	-0.03	0.12	-0.11	-0.13	3.41	0.20	-0.86	0.96	1.22	-0.43
16/06	21/06	-0.34	-0.24	-0.64	-0.65	3.00	-0.37	-0.26	-0.69	-0.71	2.74	0.58	0.41	1.20	1.35	-1.63
17/06	22/06	-0.58	-0.47	-0.96	-0.97	2.80	-0.63	-0.51	-1.05	-1.05	2.56	0.81	0.67	1.52	1.74	-1.81
18/06	23/06	-0.55	-0.47	-1.06	-1.07	2.75	-0.59	-0.51	-1.13	-1.14	2.57	0.72	0.63	1.56	1.83	-1.90
19/06	24/06	-0.62	-0.59	-1.33	-1.33	2.57	-0.67	-0.63	-1.42	-1.41	2.41	0.59	0.58	1.45	1.67	-2.42

Report Ends